^{18}F RADIOLABELING

OF

EPIDERMAL GROWTH FACTOR RECEPTOR-TYROSINE KINASE INHIBITOR ANTI-CANCER DRUGS

FOR

THERAPEUTIC OUTCOME STUDIES

A Thesis

Presented to

The Faculty of Graduate Studies

of

Lakehead University

by

Karissa Kilby

In partial fulfillment of the requirements for the degree of

Master of Science

January 19, 2023

ABSTRACT

^{18}F RADIOLABELING

OF

EPIDERMAL GROWTH FACTOR RECEPTOR-TYROSINE KINASE INHIBITOR ANTI-CANCER DRUGS

FOR

THERAPEUTIC OUTCOME STUDIES

Karissa Kilby — Supervisor

Lakehead University — Dr. M. Campbell

Epidermal growth factor receptor is a transmembrane protein with tyrosine kinase activity that plays a vital role in the proliferation, differentiation, and survival of normal cells. When mutations in this protein occur, they can cause cancer in which there is currently no cure. Epidermal growth factor receptor-tyrosine kinase inhibitor anticancer drugs are available to treat the cancer and allow progression free survival. Not all patients will benefit from this targeted therapy and therefore knowing the mutation status before administering EGFR-TKIs is important. PET imaging can be used to determine level of expression and mutation status instead of repeated invasive biopsies. The problem with these drugs is that resistance is typically seen within 18 months from the start of treatment, therefore this project aims to develop a tracer to be used with positron emission tomography imaging for therapeutic outcome studies to monitor resistance of these drugs in patients. Although patients will develop resistance, it is important to know when resistance is seen. The first part of this project aimed to synthesize an ^{18}F analogue

of erlotinib, a first-generation epidermal growth factor receptor-tyrosine kinase inhibitor anticancer drug. This synthesis was unsuccessful as it was unable to yield pure products in an efficient manner. The second part of the project aimed to synthesize a model system that models epidermal growth factor receptor-tyrosine kinase inhibitor anticancer drugs. This model system will be used to develop a synthetic strategy to be able to radiolabel all of the drugs using a single protocol. This project was unsuccessful at producing a viable model system due to problems in tosylation and fluorination reactions. The third part of the project aimed to use the synthetic strategy used to build the model system to make an ^{18}F analogue of erlotinib. This project was not completed due to lack of success in synthesis of a viable model system as well as time constraints. All successful reactions were purified and characterized using mass spectrometry, proton nuclear magnetic resonance, carbon nuclear magnetic resonance and some by infrared spectrometry.

ACKNOWLEDGEMENTS

I would like to sincerely thank my supervisor, Dr. Campbell, for his support and guidance throughout my entire project. A second thanks goes to Dr. Floriano and Dr. Hou for agreeing to be on my committee, as well as Dr. Gottardo for stepping up to be an alternate committee member last minute. Further thanks go to Jessica Allingham for her advice, guidance, and assistance throughout this process. I would also like to thank Mitacs for providing funding to do part of my project abroad. I would also like to thank Dr. Pichler, Dr. Mauer, and all of the members of the lab group at the Werner Siemens Imaging Center in Tübingen, Germany, for hosting me as part of the Mitacs scholarship and assisting me in any way they can. Finally, I would like to thank my friends and family for their endless love and support.

TABLE OF CONTENTS

LIST OF FIGURES

LIST OF SCHEMES

LIST OF EQUATIONS

LIST OF ABBREVIATIONS

Ac_2O	Acetic Anhydride
α	Alpha
ATP	Adenosine Triphosphate
β^-	Beta Minus
β^+	Beta Plus
^{11}C	Carbon-11
^{13}C NMR	Carbon-13 Nuclear Magnetic Resonance
CuI	Copper Iodide
DCM	Dichloromethane
DIPEA	Diisopropylethylamine
DMAP	4-dimethylaminopyridine
DMF	N,N-Dimethylformamide
DMSO	Dimethyl Sulfoxide
DNA	Deoxyribonucleic Acid
EGF	Epidermal Growth Factor
EGFR	Epidermal Growth Factor Receptor
EGFR-TKI	Epidermal Growth Factor Receptor-Tyrosine Kinase Inhibitor
Et_2NH	Diethylamine
^{18}F	Fluorine-18
^{19}F	Fluorine-19
FEtTs	2-fluoro p-toluenesulfonate
^{18}F-FDG	^{18}F-Fluorodeoxyglucose

^{18}F-FDG-6-P	^{18}F-fluorodeoxyglucose-6-phosphate
^{1}H NMR	Proton Nuclear Magnetic Resonance
HER	Human Epidermal Growth Factor Receptor
IR	Infrared Spectroscopy
iPrOH	Isopropanol
K_2CO_3	Potassium Carbonate
LCMS	Liquid Chromatography Mass Spectrometry
Li_2CO_3	Lithium Carbonate
MS	Mass Spectrometry
^{13}N	Nitrogen-13
NaH	Sodium Hydride
^{15}O	Oxygen-15
^{18}O	Oxygen-18
$Pd(PPh_3)_2Cl_2$	bis(triphenylphosphine)palladium (II) dichloride
PDB	Protein Data Bank
PET	Positron Emission Tomography
PTB	Phosphotyrosine Binding
RCSB	Research Collaboratory for Structural Bioinformatics
SH2	Src homology domain 2
TGF-α	Transforming Growth Factor - α
TLC	Thin Layer Chromatography
TsCl	p-Toluenesulfonyl Chloride
YASARA	Yet Another Scientific Artificial Reality Application

λ	Lambda; Nuclide Decay Constant
γ	Gamma Radiation

CHAPTER 1: BACKGROUND INFORMATION

1.1 EPIDERMAL GROWTH FACTOR RECEPTOR AS A TARGET FOR ANTI-CANCER DRUGS

1.1.2 EPIDERMAL GROWTH FACTOR RECEPTOR

Epidermal growth factor receptor (EGFR) is a 170-kDa transmembrane glycoprotein with tyrosine kinase activity (**Figure 2**).[1] It transmits growth-inducing signals to cells stimulated by an EGFR ligand and is part of the ErbB receptor family of tyrosine kinase receptors. This family consists of four members, ErbB 1 (termed EGFR and HER1), ErbB 2 (termed HER2 or Neu), ErbB 3 (termed HER3), and ErbB 4 (termed HER4); where HER stands for human epidermal growth factor receptor. This family of receptors plays a vital role in the proliferation, differentiation, and survival of healthy cells.[2] Structurally the ErbB family of receptors consists of a cysteine-rich extracellular N-terminal ligand-binding domain with a dimerization arm, a hydrophobic transmembrane domain, and an intracellular, highly conserved cytoplasmic C-terminal tyrosine kinase domain containing several phosphorylation sites. EGFR has an extracellular epidermal growth factor (EGF) binding domain and an intracellular tyrosine kinase domain that regulates signalling pathways to control cellular proliferation.[1][4] The extracellular domain is subdivided into four domains referred to as I, II, III, and IV which is depicted in **Figure 1**. The extracellular domain also exists in both closed, inactive and open, active forms. In the closed form, domains II and IV interact with each other preventing I and III to be able to interact with the EGFR ligands. In the open form, II and IV move away from each other allowing I and III to expose their binding pocket allowing ligand binding and dimerization.[5] In normal tissues, the activation of EGFR by available EGFR ligands is highly regulated to ensure that cell proliferation kinetics match the tissue's requirements to meet homeostasis.[3]

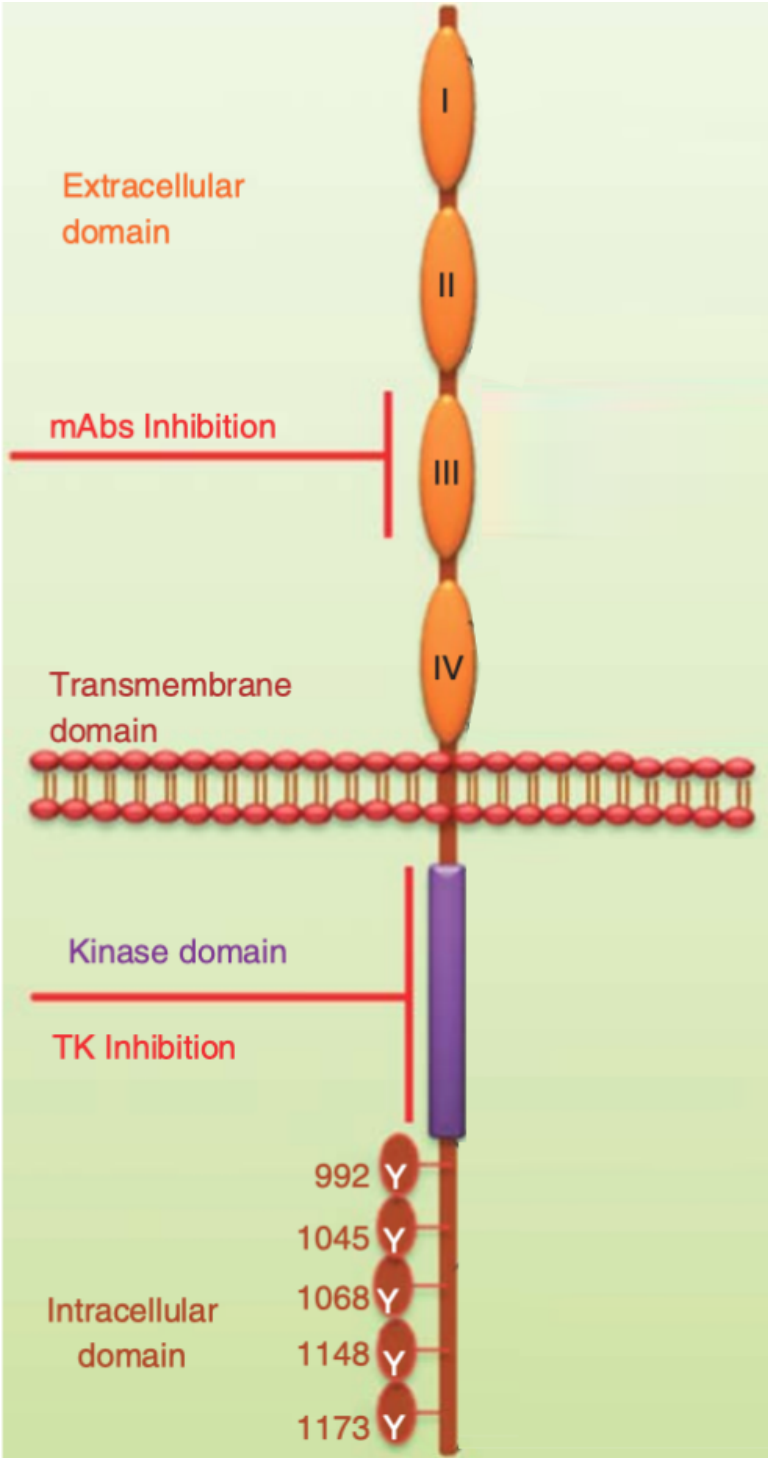

Figure 1: General Structure of Members of the ErbB Receptor Family[5]

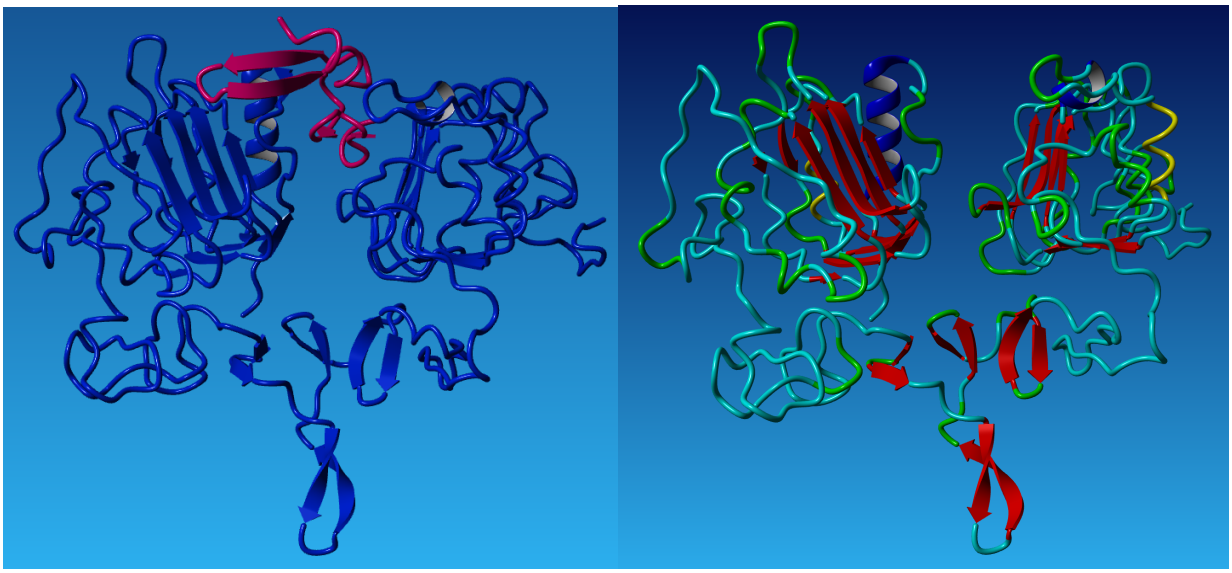

Figure 2: Crystal structure of epidermal growth factor receptor bound and unbound to epidermal growth factor. Protein data bank (PDB) code 1IVO. The structure was retrieved from RCSB PDB[6] and rendered by using YASARA.[7]

When EGF or transforming growth factor α (TGF-α), which are EGFR ligands, bind to EGFR it is activated. EGF is a 53 amino acid long polypeptide with a molecular weight of ~6 kDa and can stimulate cell growth and differentiation by binding to EGFR.[1] This causes EGFR to form a homodimer with a neighbouring EGFR or a heterodimer with a neighbouring member of the ErbB receptor family. The EGFR dimerization stimulates tyrosine kinase activity which causes intracellular autophosphorylation of six tyrosine residues found on the C-terminus of EGFR. The autophosphorylation sites are located in the non-catalytic tail of the receptor, and they recruit various adapter proteins with Src homology domain 2 (SH2) or phosphotyrosine binding (PTB) domains. EGFR can phosphorylate target proteins and can be phosphorylated by other kinases. Autophosphorylation allows further downstream signalling by proteins associated with the phosphorylated tyrosines, allowing for downstream activation of several signal transduction cascades. EGF/EGFR signalling pathway is one of the most important signalling pathways in mammalian cells (**Figure 3**). It regulates important events, including cell

proliferation, migration, differentiation, apoptosis, and intracellular communication.[1][8] After the cell signalling is complete, two pathways are possible. The first is that the receptor can be internalized into the cell and tagged for degradation. The receptor is taken in by the cell through invagination of the cell membrane into an endosome, then the receptor is degraded. The second possible outcome is that EGF or TGF-α bound to the receptor can dissociate in the early endosomal stage, and EGFR can be recycled.[8]

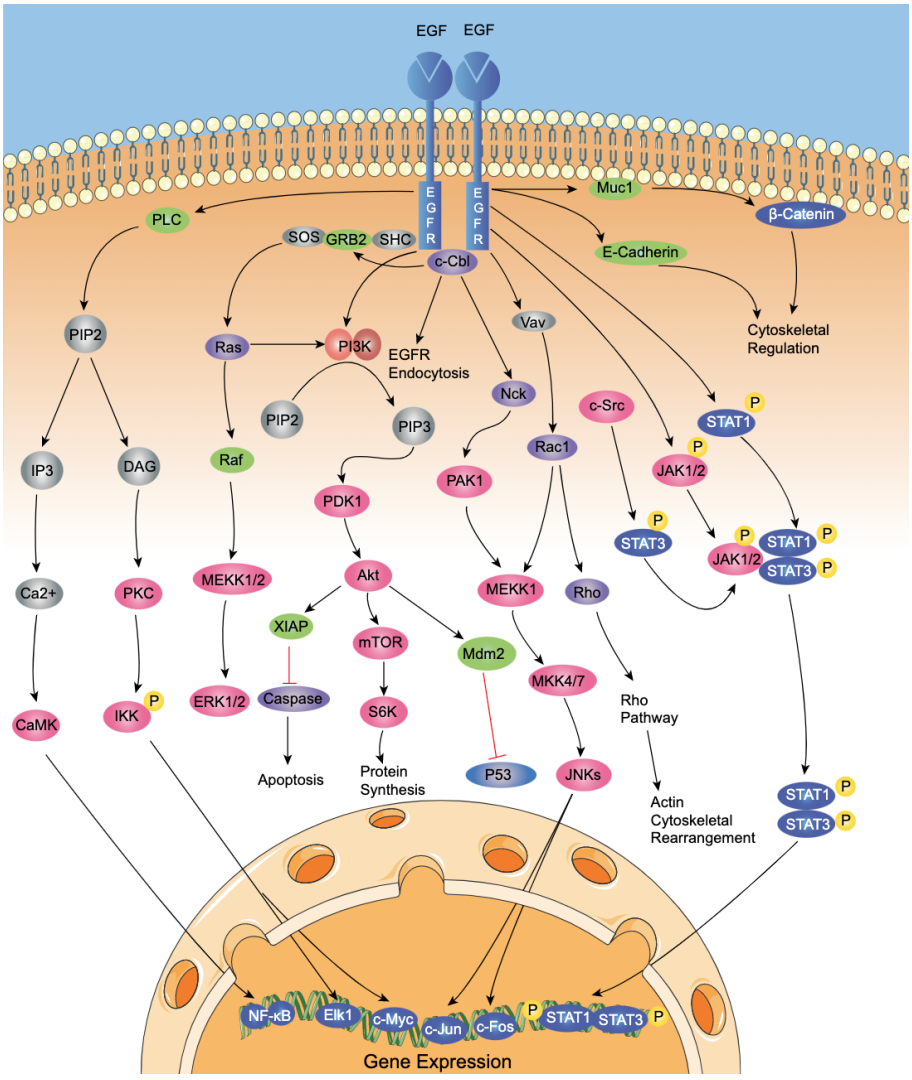

Figure 3: Signalling pathways of EGF/EGFR[1]

1.1.2 EPIDERMAL GROWTH FACTOR AND CANCER

Cancer is a group of more than 100 diseases that develop over time in the human body. It involves the uncontrolled division of cells and can develop in any part of the body, each with unique features and biochemical processes. Cancer begins when a cell's normal cell division and termination programming fails, forming a mass. Tumors threaten an individual's life when the growth disrupts the tissues and organs in the body needed for survival.[9] Cancer affects millions of people worldwide every year, with an estimated 18.1 million cases and 9.6 million deaths and approximately 90% of deaths from cancer is from metastasis. One in five men and one in six women will develop cancer in their lifetime.[10] Modern medicine has allowed millions of people to be cured and individuals with cancer to live longer than ever before. Even with the advances in modern medicine, millions of people still die of cancer each year. There are many different drugs available to treat various cancers. One problem is that the drugs are not always effective at fighting the intended cancer, or the cancer becomes resistant to the drug over time. Many cancers respond to traditional chemotherapy, but only a limited number of cancers can be cured. Resistance to drugs can develop due to numerous biochemical processes dependent on the structure and mechanism of the drug, and multi-drug resistance is a significant challenge in treating cancer. New, more targeted therapies are being developed, and the use of biomarkers plays an increasingly important role in the treatment of cancer patients.[10]

In healthy cells, the expression of EGFR ranges from 40,000 to 100,000 receptors per cell; overexpression of EGFR is common in solid tumor cancers. These cancers include breast cancer, head and neck cancer, non-small cell lung cancer, bladder cancers, and pancreatic cancers. In these types of cancers, the cells can express up to 2,000,000 receptors per cell. The over expression produces excess signal generation and activation of downstream signalling,

resulting in uncontrolled growth.[4] EGFR signalling is consistently active due to genetic mutation, genetic amplification, or both; the overactivation mutations are found in the tyrosine kinase domain of EGFR. More than 90% of the known mutations are deletions of exon 19 and point mutations of exon 21. An exon is the part of the deoxyribonucleic acid (DNA) sequence that is expressed in the final protein, and a point mutation is a genetic mutation in which a single nucleotide is altered, deleted, changed, or inserted.[11] When the deletion of exon 19 or point mutation of exon 21 is present, EGFR is consistently stimulated causing uncontrolled growth. This can be from the production of EGFR ligands in tumor microenvironments or EGFR getting locked in a constant activation state. The increased EGFR activity enhances tumor growth, invasion, and metastasis, resulting in very aggressive cancers.[12] The effects of downstream signalling caused by mutated EGFR is demonstrated in **Figure 4**, these include angiogenesis effects, growth effects, and cell motility and metastasis.[4]

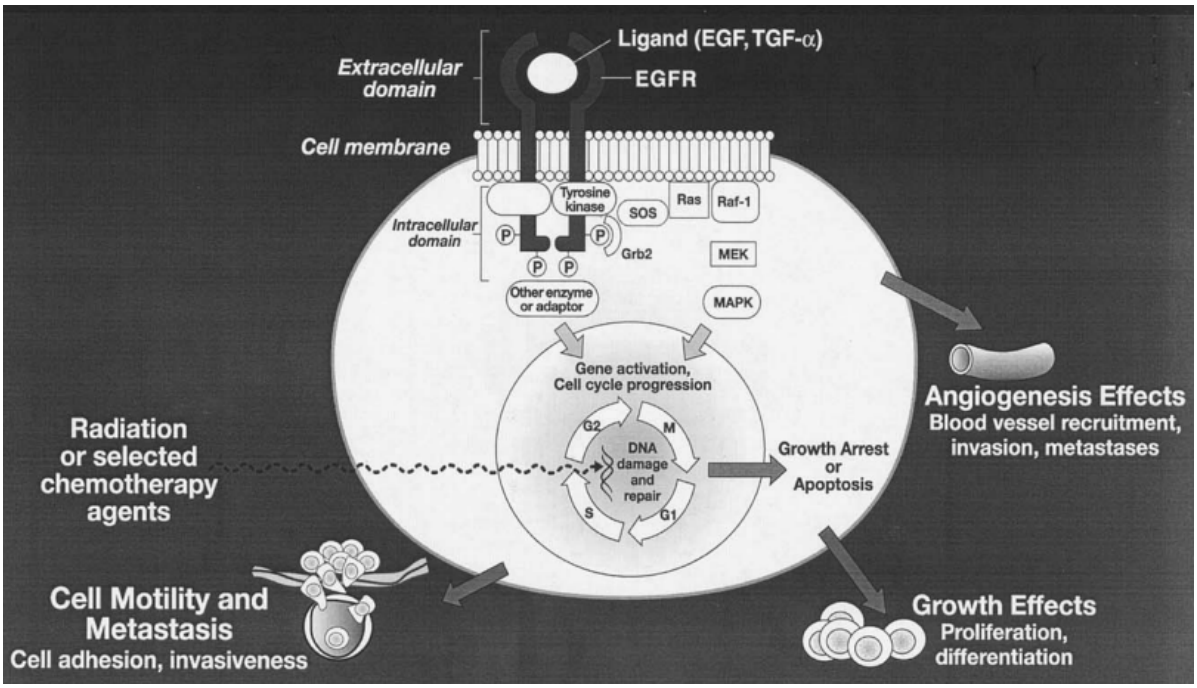

Figure 4: Schematic representation of EGFR's downstream signalling of tumor growth and metastasis.[4] Copyright privileges obtained from copyright holders.

1.1.3 TREATMENT FOR EPIDERMAL GROWTH FACTOR RECEPTOR MUTATION POSITIVE CANCERS

Currently there are no long-term treatments or cures for cancers caused by EGFR mutations. Even though this is the case, there are treatments available to prolong life including surgery, traditional platinum-based chemotherapy, and targeted therapies.[13] The targeted therapies consist of a family of epidermal growth factor-tyrosine kinase inhibitors (EGFR-TKIs); they are routinely used to treat the cancers caused by EGFR mutations. The drugs are used as first-line therapy against cancers positive for EGFR mutations and significantly improve progression-free survival, objective response rate, and quality of life compared to conventional platinum-based chemotherapies.[11] There are three generations of EGFR-TKIs; the first-generation drugs bind to both mutated and wild-type EGFR in cells, but they have a higher affinity for the mutated EGFR. The goal of the first-generation EGFR-TKIs is to block the activation of downstream signalling of EGFR by binding to the adenosine triphosphate (ATP) binding sites[11] which causes reduced downstream signalling in EGFR.[13] These first-generation EGFR-TKIs include erlotinib, gefitinib, and icotinib (**Figure 5**); which are small, orally available molecules that reversibly inhibit the kinase activity of EGFR [14][15]. One issue with the first-generation EGFR-TKIs is that the tumors always become resistant to these drugs. The resistance is caused by the T790M mutation in over 50% of the cases.[16] This mutation is a substitution of threonine with methionine at position 790 of exon 20; and affects the ATP binding pocket of the EGFR kinase domain and sterically hinders the binding of the first-generation EGFR-TKIs.[16] It also increases affinity to ATP over the EGFR-TKIs.[15]

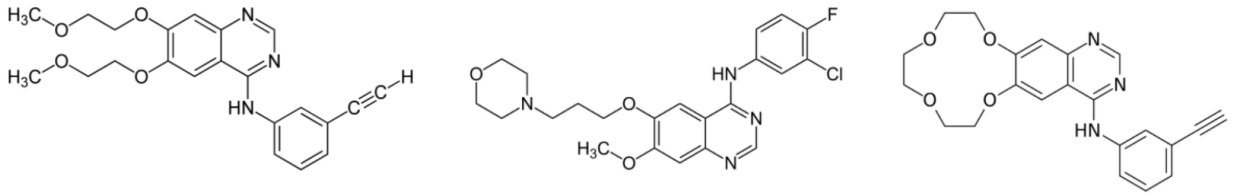

Erlotinib Gefitinib Icotinib

Figure 5: Structures of first-generation EGFR-TKIs gefitinib, erlotinib, and icotinib.

Second-generation EGFR-TKIs are irreversible inhibitors of autophosphorylation of ATP in the ATP binding site on EGFR. These drugs were developed to overcome the resistance due to the failure of the first-generation EGFR-TKIs.[11] These drugs can overcome the developed resistance to first-generation EGFR-TKIs and include the drugs afatinib, dacomitinib and neratinib (**Figure 6**). EGFR has a higher affinity for these second-generation drugs compared to ATP and are more favourable because they are irreversible inhibitors. This allows for more persistent suppression of EGFR signalling as well as reducing the dosage.[17] Even though these drugs are better at overcoming resistance due to the irreversible mechanism compared to the first-generation EGFR-TKIs, EGFR still mutates and develops resistance to favour ATP over these drugs.[11] Another issue is that approximately 20–30% of patients with EGFR mutated cancers will not respond to first and second generation EGFR-TKIs because they have intrinsic, or primary resistance. This means that the cancer is already resistant to the drugs before treatment has even begun.[19]

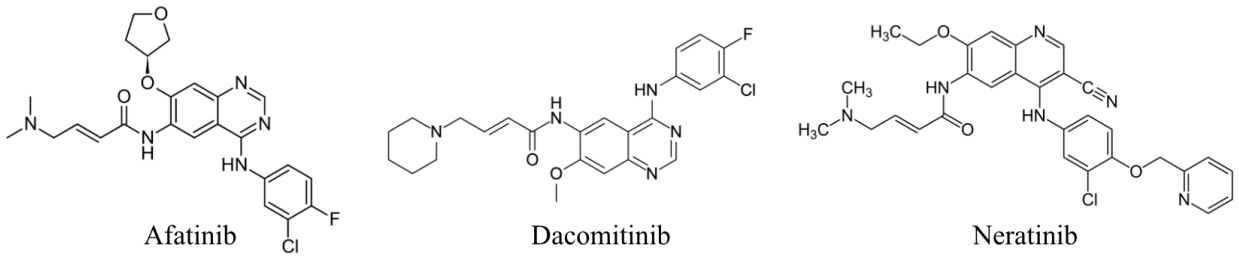

Figure 6: Structure of second-generation EGFR-TKIs afatinib, dacomitinib, and neratinib.

First- and second-generation EGFR-TKIs are structurally similar. They all contain a quinazoline, with the nitrogen on the 4-position of the quinazoline connected to a substituted aromatic ring, as well as varying solvent exposed side chains. **Figure 7** demonstrates structure identification regions of these compounds. These drugs mimic ATP because the goal of these drugs is to be a competitive inhibitor to ATP in order halt downstream signalling which causes tumor progression and metastasis. The quinazoline with the amine is modeled after the adenine structure in ATP and the side chains are modeled after the triphosphate coming off the ribose. **Figure 8** illustrates the structural similarities between ATP and EGFR-TKIs. The EGFR-TKIs bind to EGFR via hydrogen bonding of a nitrogen in the quinazoline to methionine 793 in the protein. **Figure 9** is a two-dimensional representation of how EGFR-TKIs bind to the ATP binding pocket in EGFR using gefitinib as an example.[19]

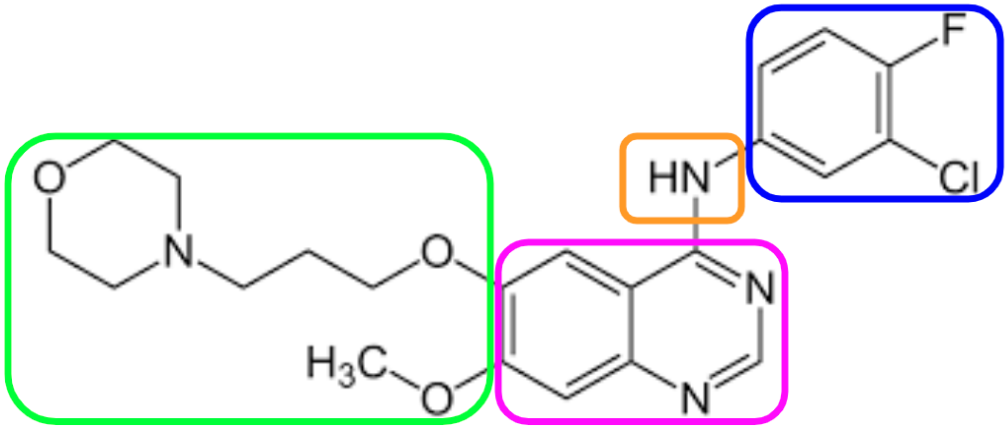

Figure 7: Identification of Structural Components of First- and Second-Generation EGFR-TKIs. Green represents the varying solvent exposed side chains, pink represents the quinazoline, blue represents the substituted aromatic ring, and orange represents the nitrogen linking the quinazoline with the aromatic ring.

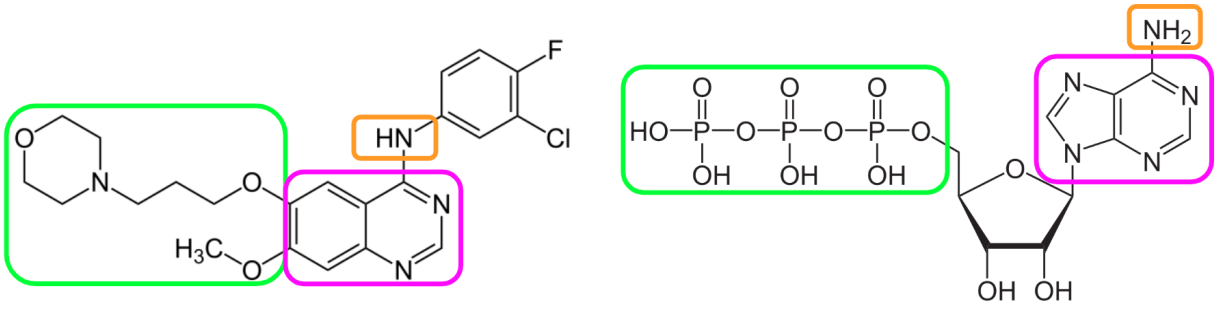

Gefitinib Adenosine Triphosphate

Figure 8: Diagram showing the structural similarities between EGFR-TKIs and ATP using gefitinib as an example.

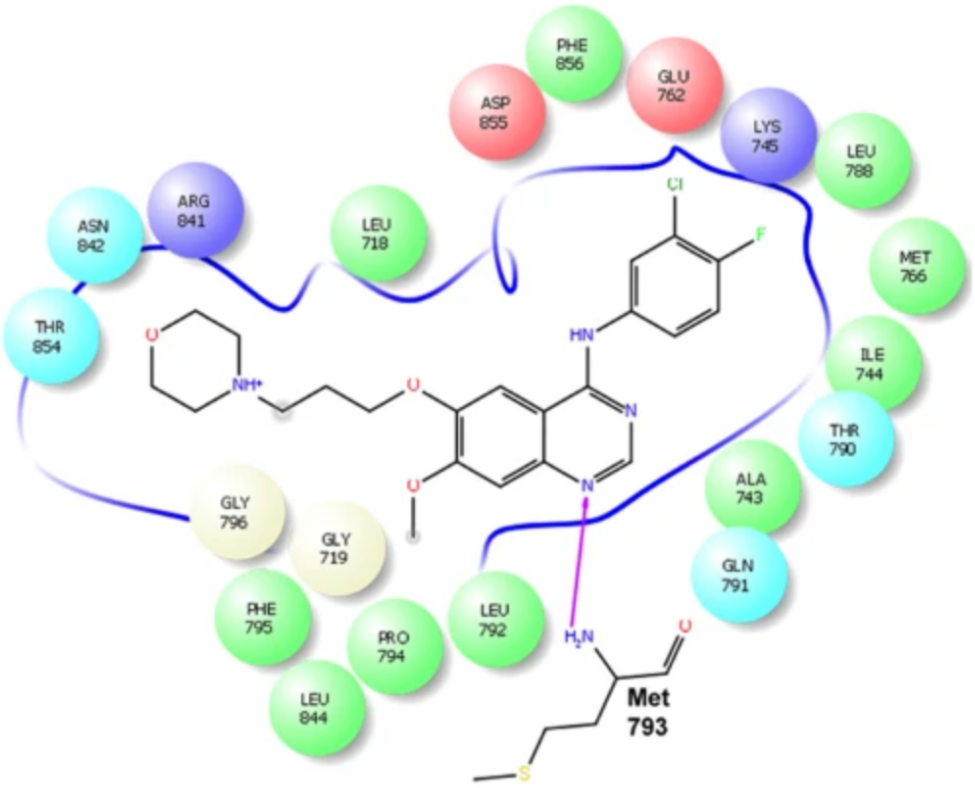

Figure 9: Two-dimensional representation of how EGFR-TKIs bind to the ATP binding site found in EGFR. The hydrogen bonding between the quinazoline nitrogen and methionine 793 is shown by the purple arrow.[19]

Third-generation EGFR-TKIs (**Figure 10**) are mutant selective and structurally different from both first and second-generation drugs. These drugs include osimertinib, rociletinib, and olmutinib and contain a Michael acceptor that forms an irreversible covalent bond to cysteine 797 in the ATP binding site. They are specifically designed to bind to and inhibit EGFR with the T790M mutation without binding to wild-type EGFR. These third-generation EGFR-TKIs can treat patients with cancer progression despite being treated with first and second-generation drugs and are T790M mutation-positive.[11][14] Osimertinib has become a first line treatment as it

has better efficacy than erlotinib or gefitinib and a second line treatment for individuals whose cancer has developed the T790M mutation.[19] Unfortunately, different resistance mechanisms cause challenges for the third-generation drugs, and other drugs are currently being developed to target these new mutations.[11][14] Due to new recurring resistance patterns seen with these drugs, new kinase inhibitors are being developed which are designed to bind at allosteric sites within the autophosphorylation domain of EGFR.[34]

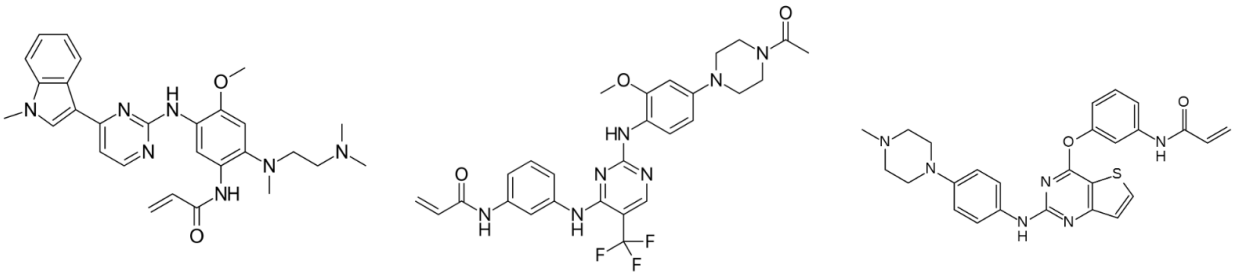

Osimertinib Rociletinib Olmutinib

Figure 10: Structure of third-generation EGFR-TKIs osimertinib, rociletinib, and olmutinib

Section 1.1 describes how mutated EGFR plays a major role in cancer formation and progression leading to very aggressive cancers, poor prognosis and short-term survival. Even though there are no cures for these types of cancers, therapies are available that are effective in slowing cancer progression and allow people to survive longer. The current first line treatments only work for 10-14 months, eventually all patient's tumors become resistant to first- and second-generation EGFR-TKIs. The patient's tumor may also have resistance before starting treatment, this leaves treatment ineffective and cancer progression imminent. There is a need for an efficient method of monitoring for drug resistance within EGFR mutated cancers. This can be done by putting a radiolabel on the drugs and conducting imaging using a technique such as

positron emission tomography (PET) to determine if the drug is binding to tumor associated EGFR. The underlying principle being that if the drug does not reach and bind to the tumor it will not be an effective treatment. The goal of this project is to design a synthetic scheme that can be applied to first- and second-generation EGFR-TKIs for efficient radiolabelling with PET isotopes to enable imaging studies to predict therapeutic outcomes. These drugs will be used in PET imaging for monitoring tumor resistance of patients undergoing treatments with EGFR-TKIs. As the treatment continues this tracer can be used to identify the onset of resistance.

1.2 RADIOCHEMISTRY

1.2.1 RADIOACTIVE DECAY

Matter is composed of atoms, an atom consists of particles called protons, neutrons, and electrons. A proton is a positively charged particle that is found in the nucleus and the number of protons designates the atomic number of the atom, a neutron is a particle found in the nucleus with a neutral charge. The mass of the atom is determined by the sum of the number of protons and neutrons and the given number of protons and neutrons in a nucleus gives an atom called a nuclide. An electron is a negatively charged particle found in orbitals around the nucleus; the number of electrons is the same as the number of protons in an atom. The electrons rotate around the nucleus in different energy shells; they are the K-shell, L-shell, and M-shell. Each shell has orbitals that designates the maximum amount of electrons in the shell.[20]

An isotope is a family of nuclides that all have the same number of protons but different numbers of neutrons which change the mass. The number of protons determines the element, and the number of neutrons determines the isotope. Some isotopes are unstable and therefore radioactive; for example, fluorine-19 (^{19}F) is a non-radioactive isotope of fluorine; it has 9

protons and ten neutrons to give a mass of 19; compared to fluorine-18 (^{18}F), which is a radioactive isotope of fluorine, has 9 protons and nine neutrons. A radioactive isotope is also called a radionuclide. Radionuclides are unstable because of an unsuitable balance of protons and neutrons in the nucleus or due to excess energy. These unstable radionuclides undergo different decay methods such as α, β^-, β^+, electron capture, or gamma decay in order to stabilize.[20] Alpha (α) particles are the nucleus of a helium atom which consists of 2 protons and 2 neutrons with a +2 charge, in alpha decay a nuclide emits an α particle causing a decrease in the atomic number by 2 and the atomic mass number by 4, the parent nuclide is changed to a different element; an example of α decay can be seen in **Equation 1**.[21]

$$^{235}_{92}U \rightarrow {}^{231}_{90}Th + \alpha$$

Equation 1: Example α decay scheme[20]

In radionuclides where the instability comes from high neutron count, beta minus (β^-) decay occurs. The unstable nuclides gain stability from emitting a β particle, this decreases the number of neutrons and increases the number of protons (atomic number) by 1 while keeping the atomic mass the same and forming an element with an atomic number 1 higher.[21] A beta particle is an electron that is emitted from the nucleus of the atom when a neutron undergoes conversion to a proton with concurrent the release of a neutrino. An example of β^- decay can be seen in **Equation 2**.

$$^{131}_{53}I \rightarrow {}^{131}_{54}Xe + \beta^- + \underline{\nu}$$

Equation 2: Example β^- decay scheme[20]

Electron capture occurs when the instability of the nuclide is due to excess protons but the energy is less than 1.022 MeV. In this type of decay, an electron from the K-shell is captured by a proton in the nucleus to produce a neutron; a neutrino is also emitted.[20] An example of this type of decay can be seen in **Equation 3**.

$$^{67}_{31}Ga + e^{-} \rightarrow {}^{67}_{30}Zn + v$$

Equation 3: Example electron capture decay scheme.[20]

In radionuclides where the instability comes from an excess of protons, positron emission may occur. A positron is an antiparticle of an electron; it has the same mass but opposite charge. Positron emission is also called beta plus (β^{+}) decay. In this decay process, a proton is converted into a neutron; this results in the emission of a positron and a neutrino. A neutrino is a particle similar to an electron, but it has no charge and a mass so small it can be considered massless.[21][22] An example of β+ decay can be seen in **Equation 4**. The positrons that are emitted from β+ decay will travel a short distance and interact with matter. Once they lose enough energy they will collide with electrons causing an annihilation event which emits two equal and opposite 511 keV photons. This annihilation event is discussed further in **Section 1.3.1**.

$$^{18}_{9}F \rightarrow {}^{18}_{8}O + \beta^{+} + v$$

Equation 4: Example β+ decay scheme for fluorine 18[20]

When radionuclides undergo decay via α, β^{-}, β^{+}, or electron capture there is residual energy in the nucleus resulting from these processes. This causes the nucleus to be in an excited

state; the excited nuclei cannot remain in an excited state therefore the nuclei need to release energy. They do this by releasing gamma radiation, a photon, that is equal to the change in the energy state of the nucleus.[20]

Each radionuclide has a unique and specific half-life and a decay constant. The half-life is defined as the time required to reduce the initial activity to one half. This is determined by measuring the radioactivity of a sample at different time intervals and plotting them on a semilogarithmic scale; the slope of the line of best fit represents the decay constant (λ) of that atom.[20] The decay constant is the probability of decay per unit time, this value is constant and is time-independent, meaning the value will not change over time.[23] The initial activity and half its value are determined from a line of best fit and the difference between the times of the initial and half activity is the half-life. If a radioisotope has a half-life of 20 days, that means that half of its atoms have decayed after 10 days. Half-life can range from fractions of a second to millions of years and can be calculated using **Equation 5**.[20][23] The half-life equation has three terms, λ which is the decay constant, $t_{1/2}$ which is the half-life of the atom, and 0.693 which is the natural logarithm of 2. The natural logarithm of 2 is used because half-life is being calculated which means that something is being divided by 2.[20]

$$t_{1/2} = \frac{0.693}{\lambda}$$

Equation 5: Half-Life Equation where 0.693 is the natural logarithm of 2, λ is the decay constant for the atom and $t_{1/2}$ is the half-life.[20]

Radiation can exist as either particulate matter (α and β particles) or non-particulate matter (high frequency electromagnetic radiation) and both are considered forms of ionizing

radiation. Ionizing radiation is a form of energy that removes electrons from atoms of materials including air, water, and living tissue, it can travel unseen and pass through these materials. The particulate radiation passes through matter, when doing so it loses energy by interacting with electrons of atoms in the matter it is passing through. The atoms can become ionized or excited, the atom would become ionized when the electron in the interaction is ejected and the atom would become excited when the electron is raised to a higher energy state and still remains in the electron cloud. High frequency electromagnetic radiation like gamma (γ) rays interact with matter via photoelectric process, Compton scattering, and pair production. In the photoelectric process the radiation transfers its entire energy to an inner shell electron and ejects the electron. The ejected electron will be replaced by an upper shell electron and the energy difference between the 2 shells will be released. In Compton Scattering the γ radiation interacts with an outer shell electron transferring only part of its energy and ejecting the electron. The incident photon gets deflected and scattered. The scattered photon still has the ability to interact with matter. In pair production, a γ ray with an energy higher than 1.022 MeV, the photon interacts with the nucleus producing a positron and an electron and the positron will undergo annihilation.[20]

1.2.2 RADIOISOTOPE PRODUCTION

More than 3,000 nuclides are known and approximately 270 are stable. Most of the radionuclides are produced artificially using either a cyclotron or a nuclear reactor or as the decay products of other radionuclides, with ^{18}F being the most common. The cyclotron, depicted in **Figure 11**, is used to make clinically significant radionuclides like carbon-11 (^{11}C), nitrogen-13 (^{13}N), ^{18}F, and oxygen-15 (^{15}O). A cyclotron is a particle accelerator. Charged particles are accelerated in a circular path within two D-shaped electrodes called dees which are placed

between the two poles of a magnetic field under vacuum. The dees are connected to an alternating high voltage oscillator to alternate the charge of the dees, the electric field is used to accelerate the particles and the magnetic field is used to guide the particle through the dees . The charged particles used in the cyclotron can be positive ions (e.g. proton, or α particle) or negative ions (e.g. negatively charged hydrogen atom).[20] The charged particle is injected into the center of the magnet inside the dees from an ion source, the particles are attracted toward the dee with the opposite charge and while in the dee do not experience any electrical field. Each time a particle crosses from one dee to that other, the potential difference along with the change in polarity of the dee causes acceleration of the particle, as the polarity of the dees are changed the particle is repelled by the dee it is in while simultaneously attracted to the other dee causing an energy increase.[24] The increase in energy causes the particle to travel in a larger radius each time it is accelerated (each time it crosses from one dee to the other). This will continue until a maximum energy is reached and the particle will escape and be guided towards a target.[20][24]

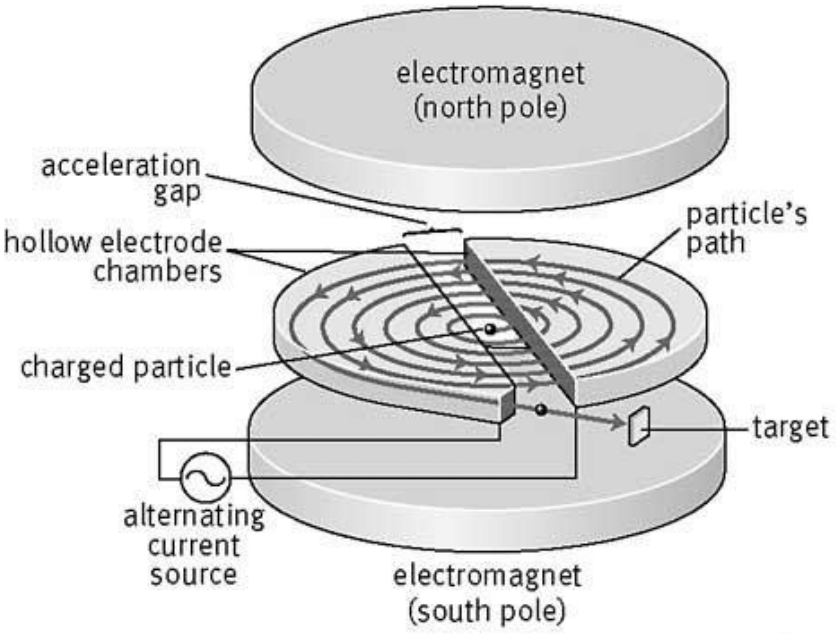

Figure 11: Diagram of particle movement in a cyclotron.[25]

^{18}F is a radioactive isotope of fluorine and is produced using a cyclotron. In the cyclotron, oxygen-18 (^{18}O) water is bombarded with an accelerated proton which converts ^{18}O to ^{18}F. See **Equation 6** for the formation of ^{18}F.

$$^{18}O + {}^{1}H \rightarrow {}^{18}F + n$$

Equation 6: Production scheme of ^{18}F

This isotope is the most commonly used radioisotope in PET tracers because of its convenient half-life, high-resolution images, high positron decay ratio, and diverse range of chemistry.[26] The half-life of 110 minutes is ideal because it is long enough to allow for the radiotracer synthesis but is short enough to decay to a safe level in the patient's body quickly. ^{18}F allows for high-resolution images because the positrons produced have a low energy of 0.635 MeV, resulting in a short diffusion range before thermalizing. This means that the positrons travel a very short distance, <2.4mm, before the annihilation event with an electron. Fluorine is a favourable atom from a medicinal chemistry aspect due to its physical properties, including high electronegativity and its ability to form a strong bond with carbon. The fluorine-carbon bond is thermally stable, oxidation resistant, and significantly stronger than a carbon-hydrogen bond. Fluorine is also a bioisostere for hydrogen based on similar size of the atoms and for oxygen based on similar size and electronegativity. Due to the many physical and radiochemical properties, and the fact that many drugs already contain fluorine, it is ideal for incorporating into small molecules to make radioligands in PET imaging.[26]

1.3 POSITRON EMISSION TOMOGRAPHY (PET) IMAGING

1.3.1 PET MECHANISM

Positron emission tomography (PET) imaging is a medical imaging modality that provides images of the biodistribution of a radiotracer *in vivo* and can be used to provide insight into biological processes in vivo.[26] PET takes advantage of the β+ decay of some radioisotopes. When a dose of a positron-emitting radioisotope is injected into the body, it will undergo decay which can be detected by ring detectors built around the patient. When a positron is emitted, it carries energy. As the positron travels, it collides with electrons in neighbouring tissues; with every collision, the positron loses energy until it is thermalized and can combine with an electron. This final collision is called an annihilation event which converts mass into energy, emitting two equal photons in opposite directions, each with an energy of 511 keV. The equal and opposite gamma rays ensure the conservation of energy and momentum is maintained. The gamma rays emitted hit a ring detector that surrounds the patient.[27] The decay process detected by a PET scanner can be seen in **Figure 12**.

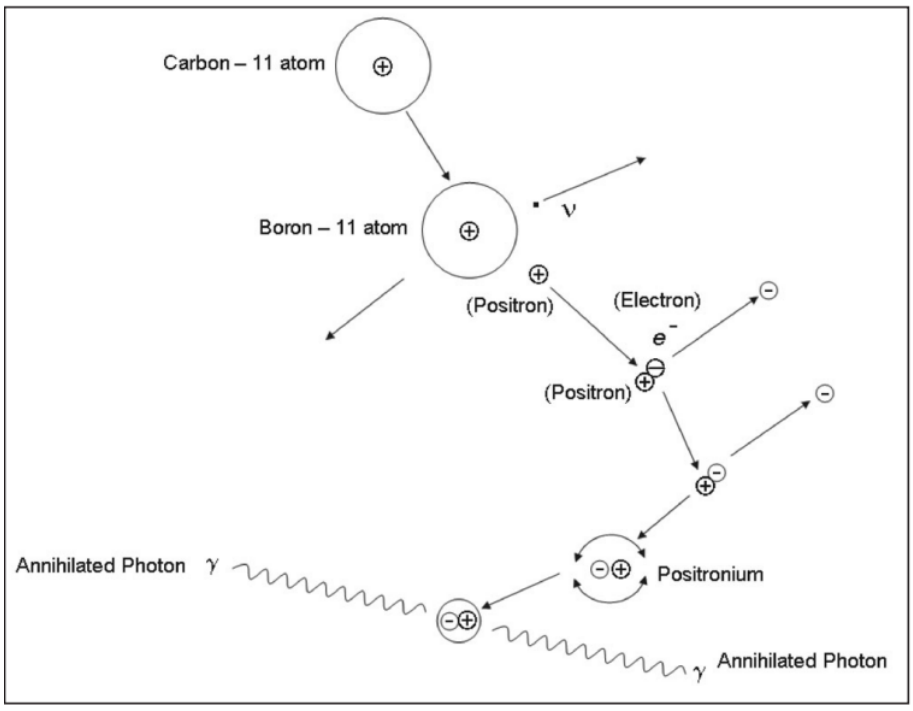

Figure 12: Schematic of beta + decay of a ^{11}C atom in PET.[28]

Copyright privileges obtained from copyright holders.

Each annihilation is considered a coincidence event; the PET detectors collect data consisting of a list of coincidence events. This is when two γ rays are detected opposite and almost simultaneously (a window of 6-12 nanoseconds). Once the data is acquired, a computer converts the collected data into an image. These images are used to study the biodistribution of the PET tracer in the patient.[20]

1.3.2 PET IN MEDICINE

PET is an imaging modality used mainly in clinical oncology; it uses radiotracers to measure many different biological processes in the body. PET has been used as a research tool, but its clinical applications have significantly grown in the last decade. Radiotracers are molecules with a radioactive label and high specificity for a target protein. Application of PET to

oncology is of growing interest and importance[29], the goals are lesion detection, characterization, staging of malignant lesions, and assessment of therapeutic response.[30] When PET is used in conjunction with suitable radiotracers, it offers the possibility to investigate and gather information on physiology, metabolism, pharmacokinetics, and pharmacodynamics.[29] It can provide a whole body image which can provide information on disease activity and spread. PET is also able to detect metabolic changes which can be used to diagnose a disease before any major anatomical changes unlike CT or MRI that detect disease at a structural level. Radiotracers used in PET can be labeled using a variety of radioactive isotopes such as ^{18}F and ^{11}C. These isotopes are positron emitters and have a short half-life. Once radiolabeled, these drugs can be injected into a patient and used with a PET scanner to determine where the drug accumulates.[26][30]

There are radiotracers that are widely used for disease diagnosis, the most common being ^{18}F-fluorodeoxyglucose (^{18}F-FDG). This molecule is an analogue of glucose and has the same transport mechanism to enter cells as glucose. Once ^{18}F-FDG enters the cells it gets phosphorylated to ^{18}F-fluorodeoxyglucose-6-phosphate (^{18}F-FDG-6-P) which does not get further metabolized and is trapped in the cells. Cancer cells have a higher rate of metabolism and glycolysis than normal cells which causes accumulation of ^{18}F-FDG-6-P than normal cells. This metabolic difference can be detected by PET imaging and is used to detect and diagnose cancer.[30]

CHAPTER 2: SYNTHESIS OF ^{18}F-ERLOTINIB ANALOGUE

2.1 SYNTHESIS PROPOSAL

As discussed in Section 1.1, EGFR mutations can cause very aggressive cancers that cannot be cured. Even though there is no cure, there are treatments available to slow progression allowing affected individuals to live longer and more comfortably. EGFR-TKIs are drugs that inhibit the activation of EGFR and are used as the first line treatment for EGFR mutation positive cancers. The main drawback associated with these drugs is that the tumors either already have or will develop resistance after 10-14 months. A way to monitor drug resistance is to develop a radioactive version of the drug to use in PET imaging.

EGFR-TKIs are widely studied, and radioactive analogues have been made using both ^{11}C, ^{18}F, ^{125}I, and ^{77}Br. Initial efforts in this project were focused on labeling erlotinib in the position indicated in **Figure 13. Scheme 1** shows the reaction scheme to get to the final product; previous analogues show that modifications of the 2-methoxyethyl chains have little impact on binding and therefore we propose to radiolabel erlotinib in the position indicated in **Figure 13.**[34] The synthesis depicted in **Scheme 1** is adapted from a reported synthesis by Zhang et al.[31]

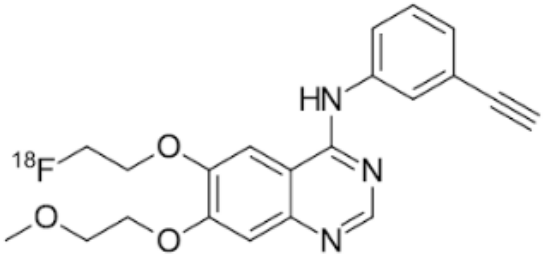

Figure 13: Proposed ^{18}F-Erlotinib Analogue, N-(3-ethynylphenyl)-6-(2-[^{18}F]fluoroethoxy)-7-(2-methoxyethoxy)quinazoline-4-amine

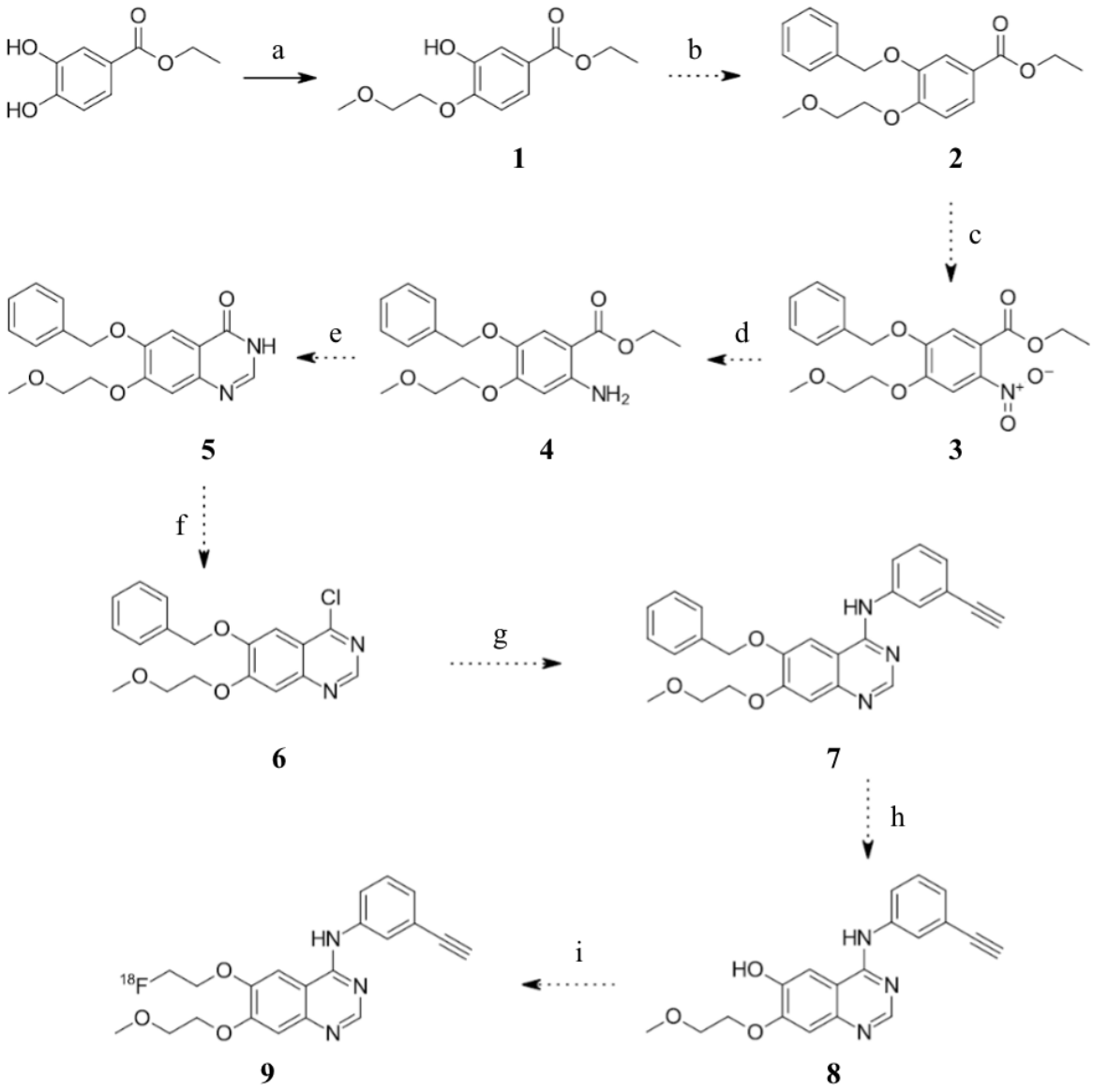

Scheme 1: Proposed synthesis of ^{18}F radiolabeled Erlotinib. (a) 1-bromo-2-methoxyethane NaH, DMF (b) benzyl bromide, K_2CO_3, CH_3CN (c) conc. H_2SO_4, conc. HNO_3, HOAc (d) Fe, HOAc (e) ammonium formate, formamide (f) phosphoryl chloride, $CHCl_3$ (g) 3-ethynylaniline, i-PrOH (h) CrO_3 HOAc (i) ^{18}F-fluoroethyl tosylate, $K_{2.2.2}$, dry CH_3CN

2.2 RESULTS AND DISCUSSION

The synthetic route proposed in **Scheme 1** encountered a number of problems. Reaction (a) of protocatechuic acid ethyl ester with 1-bromo-2-methoxyethane to yield ethyl 3-hydroxy-4-(2-methoxyethoxy)benzoate was unsuccessful. After 24 hours both thin layer chromatography

(TLC) and mass spectrometry (MS) failed to show formation of product; only the presence of starting material. This reaction was carried out based on the work of Zhang et al.[31] In order to get the reaction to proceed, potassium carbonate (K_2CO_3) was used as a base in acetonitrile (CH_3CN) and refluxed overnight. Unlike the first attempt, this attempt was successful at making the desired product, but it also yielded the other monosubstituted and disubstituted products shown in **Scheme 2**.

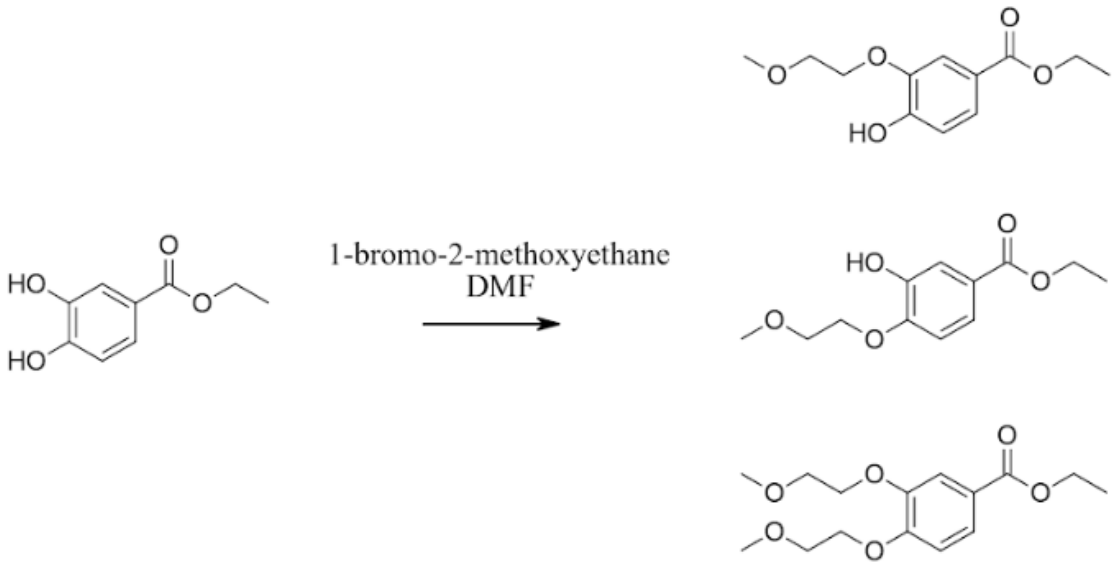

Scheme 2: Scheme depicting products obtained from reaction (a) of proposed synthesis.

The formation of the desired product was confirmed from MS and TLC analysis. Even though the desired product was synthesized, it was difficult to isolate due to the similarity of the undesired products present in the reaction mixture. Column chromatography was used to attempt to isolate the desired product, but only one or two clean fractions were obtained, and the rest gave a mixture of isotopes. Every attempt made to isolate the product in a reasonable yield was unsuccessful. Therefore, the approach to this synthesis had to be redesigned. One last effort was made to get a successful reaction, lithium carbonate (Li_2CO_3) was used as a base because it is a

weak base compared to NaH and K_2CO_3; the weaker base may be more selective in deprotonating the slightly more acidic hydroxyl group which will allow us to obtain our desired monoalkylated product. This reaction was successful in yielding the desired product, the drawback with this reaction is that it took over seven days for the reaction to proceed and even after the long reaction time, the starting material was not consumed. The long reaction times made this reaction not suitable for synthesis and another approach was needed in order to obtain the desired product with a reasonable reaction time and reasonable yield.

An alternative route was developed based on the work by Zhang et al.[31] in which the two hydroxyl groups are protected with acetyl groups. This approach allows for the synthesizing of the quinazoline and addition of the 3-ethynylaniline before modifying the side chains using the two hydroxyl groups. **Scheme 3** depicts the second approach to the synthesis of N-(3-ethynylphenyl)-7-(2-[^{18}F]fluoroethoxy)-6-(2-methoxyethoxy)quinazoline-4-amine.

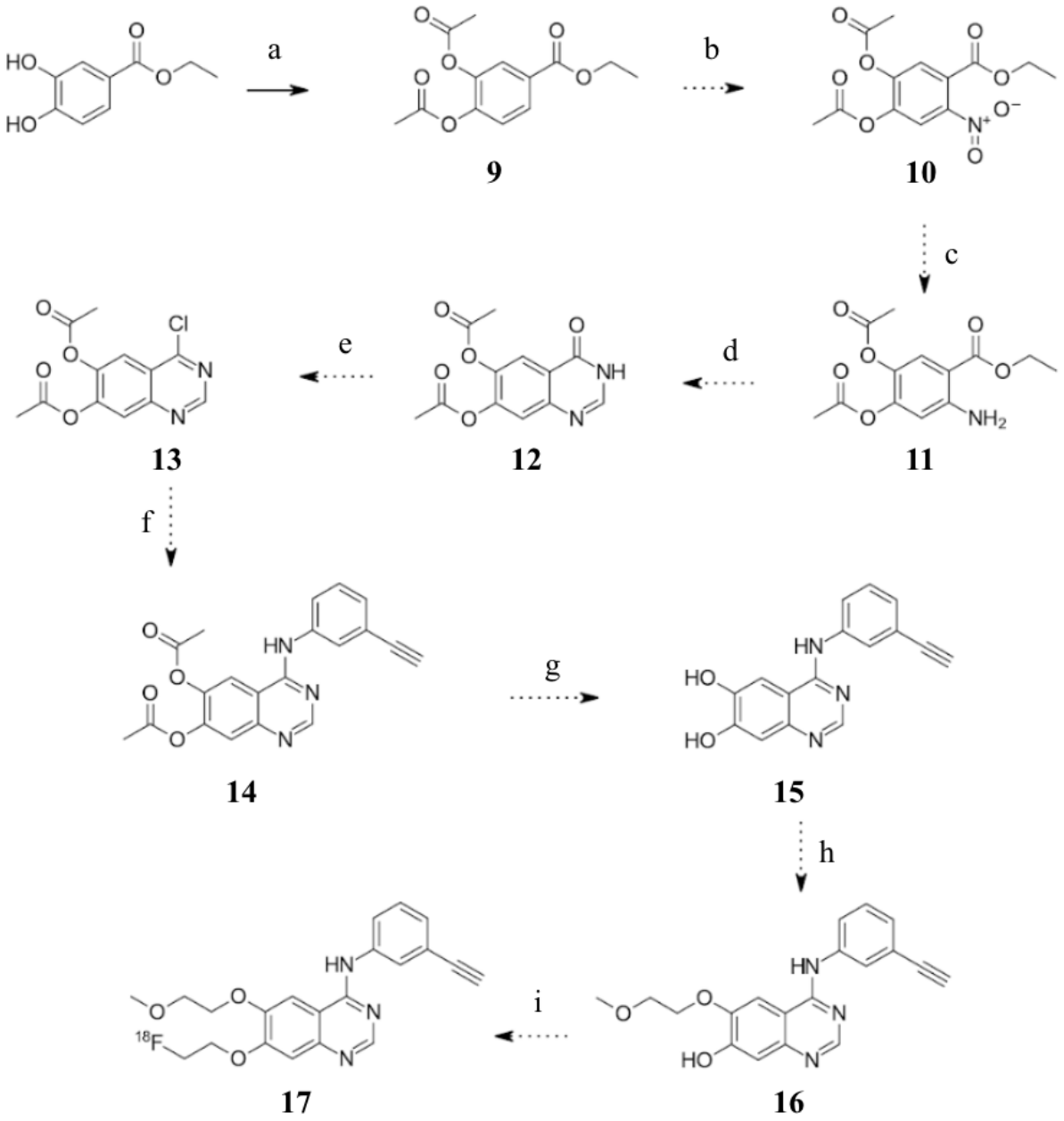

Scheme 3: Second proposed synthesis of ^{18}F labeled analogue of erlotinib. (a) Ac_2O, pyridine (b) conc. H_2SO_4, conc. HNO_3, HOAc (c) Fe, HOAc (d) ammonium formate, formamide (e) phosphoryl chloride, $CHCl_3$ (f) 3-ethynylaniline, i-PrOH (h) CrO_3 HOAc (g) MeOH, NaOMe (h) 1-bromo-2-methoxyethane, K_2CO_3, DMF (i) ^{18}F-fluoroethyl tosylate, $K_{2.2.2}$, dry CH_3CN

Reaction (a) in the second approach which combined protocatechuic acid ethyl ester with acetic anhydride (Ac_2O) in pyridine was not successful. Using the reaction conditions specified in **Scheme 3** a mixture of the monosubstituted and disubstituted products was obtained.

Characterization of the products was done using MS and TLC; on the MS, masses corresponding to both mono- and disubstituted products were identified and on TLC, multiple spots that correlate to mono- and disubstituted products were seen. Since both the mono- and disubstituted products were identified, column chromatography was used to attempt the separation of the two products which was unsuccessful. The mixture was resubjected to the reaction conditions with the purpose of pushing the reaction to completion to consume the monoacetylated product to achieve a higher yield and allow for easier separation. This was unsuccessful as the monoacetylated product would not react further to yield the diacetylated product. There is the possibility of an electronic effect which prevents formation of the disubstituted product. If an acetyl group adds to one hydroxyl group first, it may prevent the second acetyl group from adding. The absence of success synthesizing the desired product led us to revise this project which is discussed further in Chapter 3.

2.3 FUTURE WORK

This chapter discusses the attempts to synthesize a radioactive derivative of the EGFR-TKI, erlotinib. Multiple attempts at this synthesis were unsuccessful. Future work to this project would be to find a synthetic scheme that would allow for the synthesis of the desired final product, first cold using ^{19}F then to apply the synthesis to make the ^{18}F version of the product. This compound would then need to be used in binding studies to determine the ability of the tracer to be used in therapeutic outcome studies.

CHAPTER 3: SYNTHESIS OF ^{18}F LABELED EPIDERMAL GROWTH FACTOR RECEPTOR-TYROSINE KINASE INHIBITOR MODEL SYSTEM

3.1 PROPOSED SYNTHESIS

Chapter 2 discussed the first approach to this project but due to synthetic challenges, the project was altered and will be discussed in this chapter. Since all of the EGFR-TKI drugs are structurally similar, a single protocol could be developed to make ^{18}F labeled derivatives of each drug instead of developing a protocol specific to each drug. In order to develop this protocol, a model system was synthesized that contains the structural components found in all of the drugs which includes a quinazoline with an aniline bound at carbon 4. **Figure 14** shows the structure of the proposed model system. This model system will be useful in the development of the protocol as it is structurally similar to the EGFR-TKIs and can be used to experimentally determine the potential of this synthetic route before applying it to a drug. This model system also has the potential as a radiotracer for predicting therapeutic outcomes using PET. Due to the structural similarity of the first and second-generation EGFR-TKIs, they all bind in the same manner to the tyrosine kinase autophosphorylation spot on EGFR. This model system will bind in the same fashion as the drugs and has the potential to act the same biochemically. It can be a model of the EGFR-TKIs which means it has the capacity to be a tracer for resistance monitoring of patients being treated by EGFR-TKIs. **Scheme 4** shows the proposed synthetic route to synthesize the proposed model system seen in **Figure 14**.

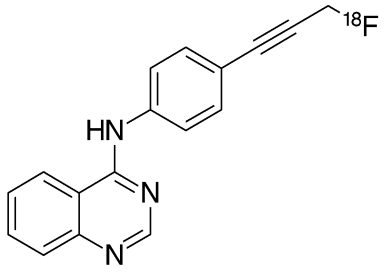

Figure 14: Proposed Structure of a Model System for Radiolabelling EGFR-TKIs

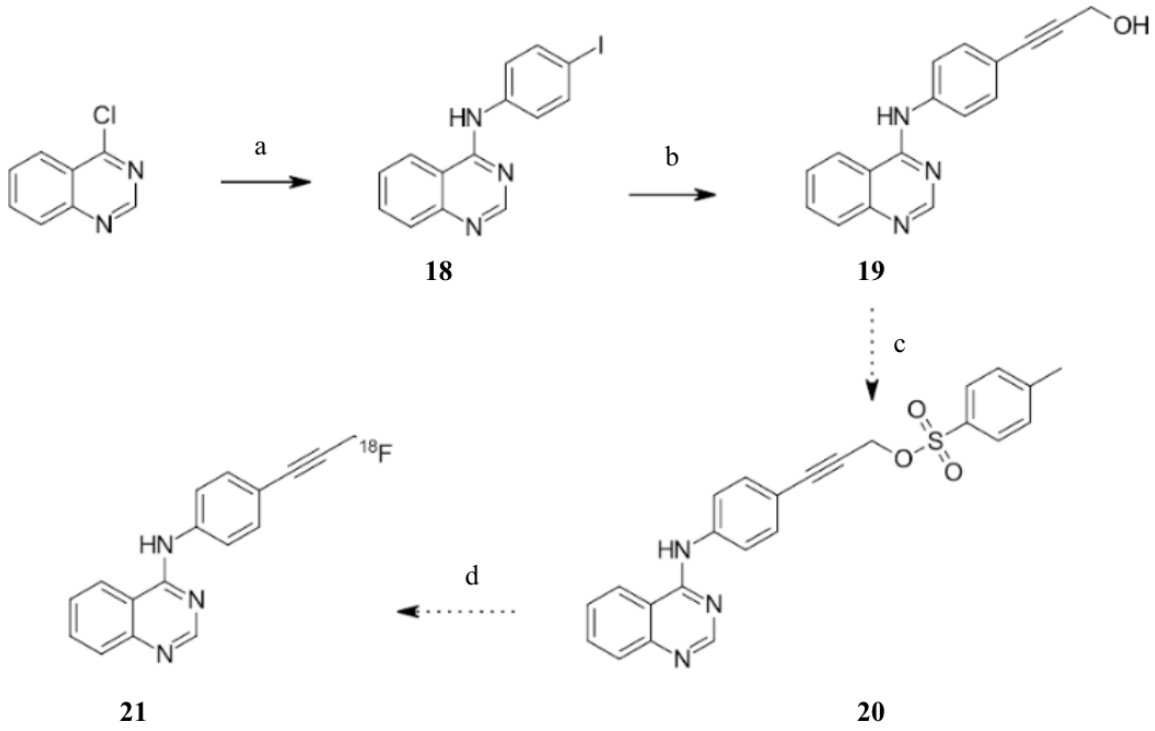

Scheme 4: Proposed synthetic route for synthesis of the proposed model system. (a) 4-iodoaniline, isopropanol (b) propargyl alcohol, $Pd(PPh_3)_2Cl_2$, CuI, Et_2NH (c) p-toluenesulfonylchloride, DIPEA, DCM (d) KF, Kryptofix 2.2.2, CH_3CN

The structure proposed in **Figure 14** was developed based on previous work done to develop EGFR PET tracers. Although lots of the drugs are substituted at the 3-position, the substitutions occur on the 4-position because 4-iodoaniline was already available and less expensive for use in the model system. In 1998, the synthesis of [O-methyl-^{11}C]PD153035 was

reported as an EGFR tracer, it is an ATP competitive tyrosine kinase inhibitor (TKI). The structure can be seen in **Figure 15.** It was shown to be selective towards EGFR tyrosine kinase when compared to other tyrosine kinases. A major limitation to this tracer is that there is uncertainty in whether the ^{11}C label is on the 6 or 7 position which makes it difficult to accurately report the structure and ability for this to be a tracer. Another limitation of this tracer is that a major metabolite of this tracer, 7-O-demethylated [6-O-methyl-^{11}C]PD153035, has a similar reported affinity as the parent compound. This means that the metabolite contributes to overall uptake in tumors as well as contributes to off target affinity. The final drawback is that this tracer is labeled using ^{11}C which has a half-life of only 20 minutes which puts limitation on synthesis, imaging time, and preventing its use in hospitals that don't have an onsite cyclotron.[34]

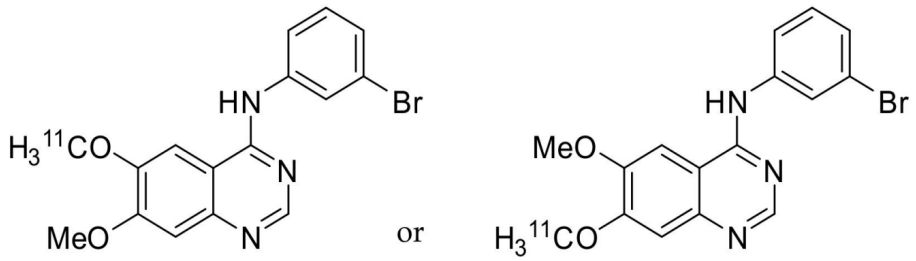

[*6-O-methyl*-^{11}C]PD153035 [*7-O-methyl*-^{11}C]PD153035

Figure 15: Structure of 6- and 7-[O-methyl-^{11}C]PD153035[34]

Other tracers reported include a group of ML- tracers shown in **Figure 16.** These tracers were developed to enable radiolabeling using ^{18}F. Studies show that N-(4-fluorophenyl)-6,7-dimethoxyquinazoline-4-amine has rapid blood clearance. After 20 minutes, only16% of the radioactivity remained in the blood. Of what was remaining, 75% was determined to be the intact

tracer. Binding studies showed that this compound was not the best candidate for a tracer. Studies on [^{18}F]ML01 showed that 36% of radioactivity in the blood could be extracted after 10 minutes after injection and only 56% of it was the intact tracer. [^{18}F]ML01 was found to have high affinity for the EGFR tyrosine kinase binding pocket but the binding affinity was too low to be a successful tracer. The next tracer developed was [^{11}C]ML03 to improve tumor retention. This tracer has an acryloyl amide which allows for irreversible binding to the tyrosine kinase domain of EGFR. Rapid blood clearance was observed and at 60 minutes post injection, 17% of the radioactivity in the blood could be extracted and of that 17%, 75% is the intact tracer. Chemically this tracer is too reactive which causes rapid *in vivo* metabolism, and this tracer is labeled using ^{11}C which has limitations in synthesis and widespread use. Derivatives of ML03 were made, called [^{11}C]ML04 and [^{18}F]ML04 to improve the bioavailability and retention. Studies on [^{11}C]ML04 show that no metabolites in blood extracts were detected and studies on [^{18}F]ML04 reveal that ML04 can inhibit EGFR expressing cell lines at low concentrations and selectively inhibit EGFR over other kinase receptors. The downside is that affinity to other macromolecules is likely the reason for it not being a successful candidate for a tracer. Other tracers developed in this family include ML04-PEG$_4$-[^{18}F]F and [^{11}C]ML04-PEG$_4$-OH. In these tracers, polyethylene glycol chains were introduced to improve solubility and reduce lipophilicity while retaining irreversible binding capabilities. The studies done were not able to accurately predict the ability of this tracer and more work needs to be done.[34]

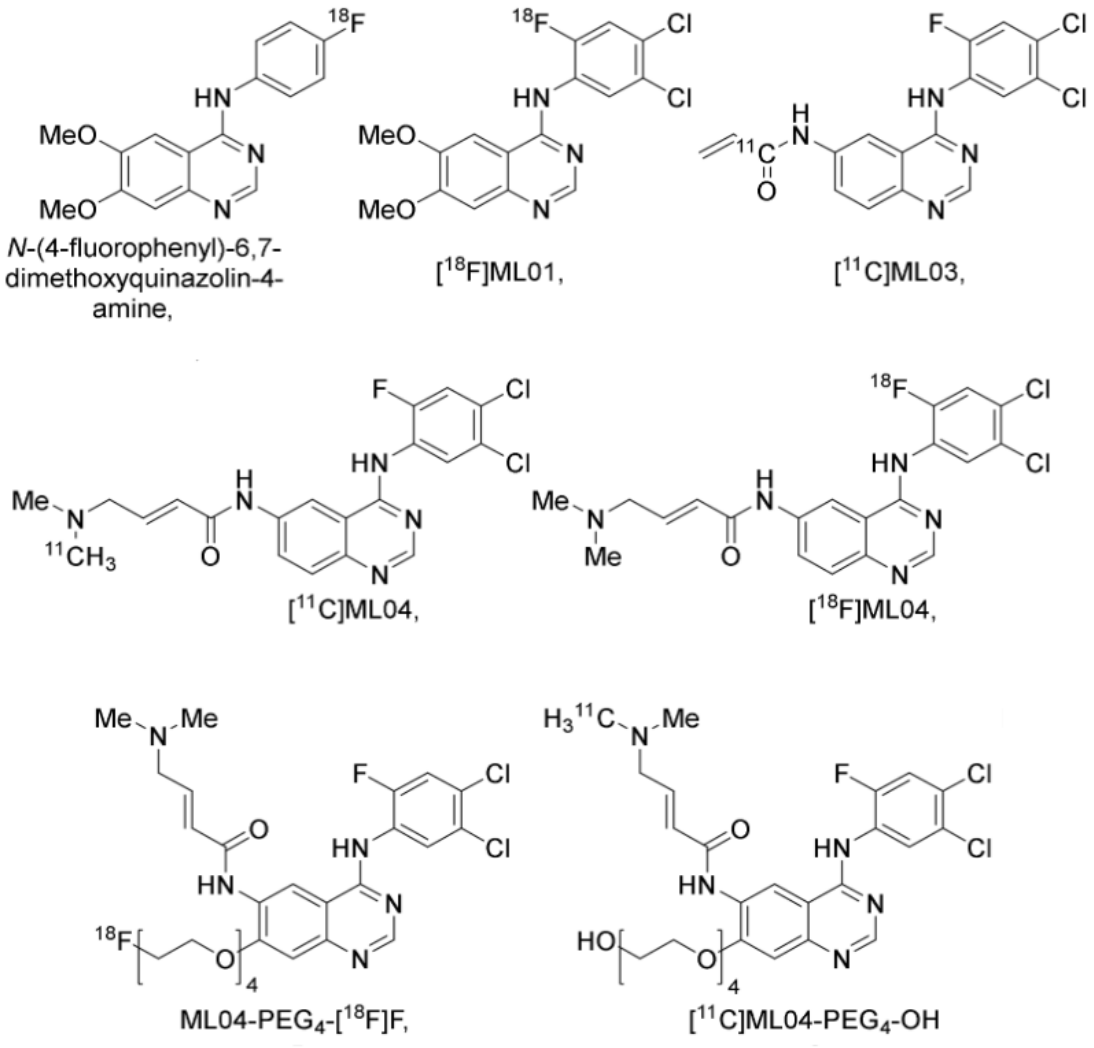

Figure 16: Structures of the ML- Series of EGFR-TKI Tracers[34]

Another group of tracers developed are the IPQA tracers that can be seen in **Figure 17.** [^{124}I]IPQA-PEG$_4$-OH is a derivative of ML04-PEG compounds, the new compound is labeled using ^{124}I. Studies done with this tracer show that tumor uptake was less than the background concentration in the 2 tumor types studied. The second tracer, [^{18}F]IPQA-PEG$_6$-F, has a ^{18}F labeled polyethylene glycol chain. This tracer was shown to inhibit mutant EGFR kinases over resistance mutated and wild type EGFR kinases and the tracer uptake could be reduced by blocking with gefitinib. In order to lower the lipophilicity and reduce the hepatobiliary clearance,

a modification was made on the 6-position resulting in the tracer morpholino-[^{124}I]IPQA. Studies on this tracer show that it is able to inhibit the EGFR phosphorylation with high potency and is a suitable imaging agent for distinguishing EGFR tyrosine kinase activating mutations.[34]

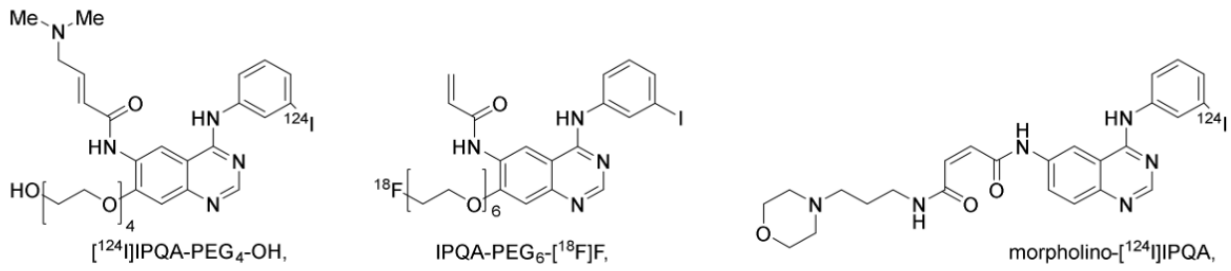

Figure 17: IPQA Series of EGFR-TKI Tracers[34]

Other PET tracers developed include derivatives of PD153035, gefitinib, erlotinib, icotinib, afatinib and rociletinib. An analogue of PD153035 was made by adding a ^{18}F labeled polyethylene glycol chain on position 7, this tracer is called [^{18}F]MPG and can be seen in **Figure 18.** This tracer is seen to preferentially inhibit Del19 EGFR mutation positive cancers. Another analogue of PD153035 is a tracer called [^{18}F]APP-1 (**Figure 18**); this tracer was developed in an attempt to differentiate between primary and secondary EGFR TK mutations. This tracer showed a binding preference for primary mutation positive EGFR compared to secondary mutation positive EGFR.[34]

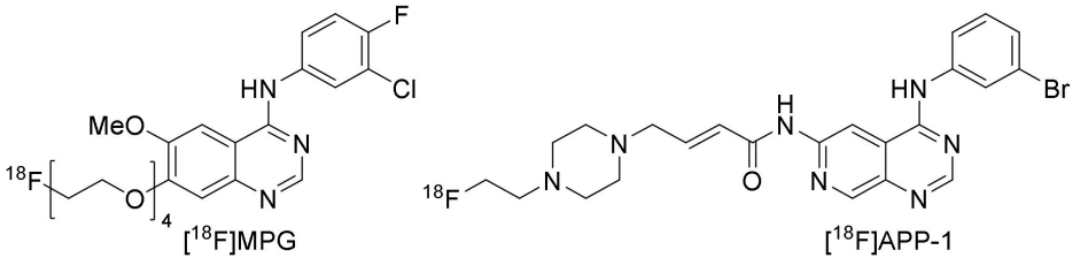

Figure 18: EGFR-TKI Tracers that are analogues of PD153035.[34]

There is one tracer that has been developed that is a derivative of gefitinib. This tracer is [^{18}F]F-IRS (**Figure 19**) which contains a radiofluorinated polyethylene glycol chain at position 7. Gefitinib has also been labeled with ^{18}F and ^{11}C, these structures can be seen in **Figure 19**. Studies done on [^{18}F]gefitinib and [^{11}C]gefitinib both showed that the uptake of these tracers is not related to EGFR expression and that there may be non-specific binding present.[34]

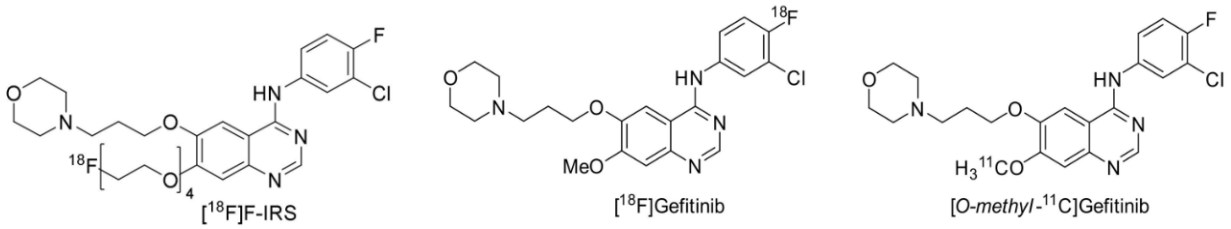

Figure 19: EGFR-TKI Tracers that are Analogues of Gefitinib[34]

Two derivatives of erlotinib have been developed, [^{18}F]F-FEA-erlotinib and 6-O-[^{18}F]fluoroethyl erlotinib [^{18}F](6-O-FEE) which can be seen in **Figure 20**. [^{18}F]F-FEA-erlotinib contains a 1-2-3,triazole scaffold replacing the terminal alkyne in erlotinib and 6-O-[^{18}F]FEE has a fluoroethyl group added to the alkyl chain at the 6-position. Erlotinib was also radiolabelled with ^{11}C on the 6-O-methyl and 7-O-methyl positions (**Figure 20**). These radiolabeled erlotinib analogues are selective to the Del19 mutation positive cancers and the selectivity of [^{11}C]erlotinib was dependent on biophysical alterations in the EGFR kinase domain due to mutation and not EGFR expression level.

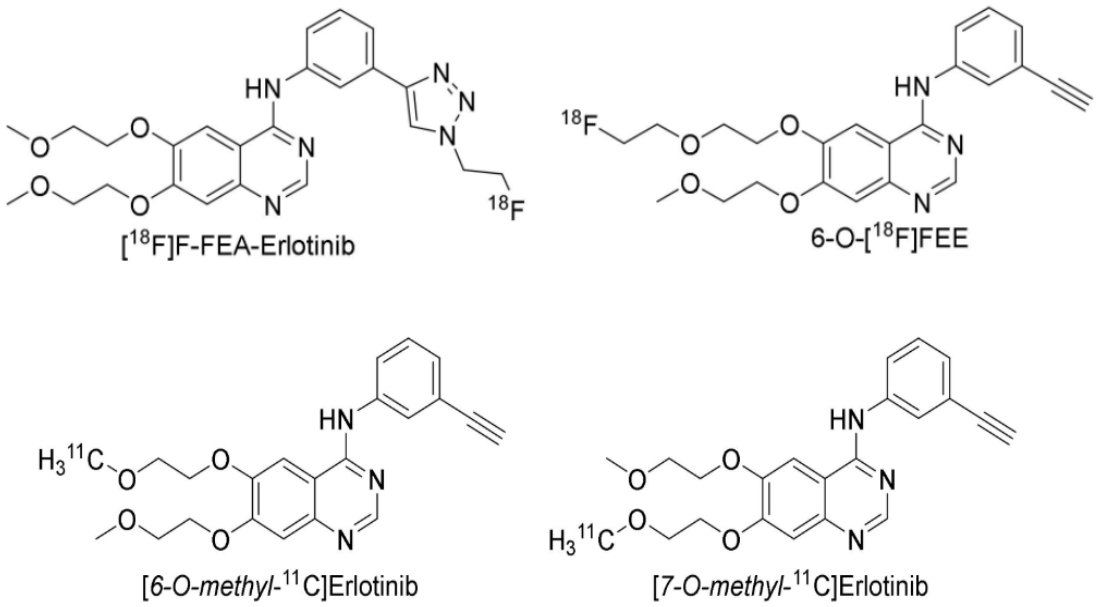

Figure 20: EGFR-TKI Tracers that are Analogues of Erlotinib[34]

There are 4 derivatives of the EGFR-TKI icotinib. They include [^{18}F]icotinib derivatives 1a, 1b, 1c, and 1d which can be seen in **Figure 21**. [^{18}F]icotinib derivatives 1a and 1c have modifications to the crown ether, derivative 1a has a smaller crown ether to reduce steric hindrance and derivative 1c has a larger crown ether to promote faster blood clearance. These derivatives also have an ^{18}F labeled fluoroethyl ether group as a replacement for the terminal alkyne. [^{18}F]icotinib derivative 1c has an ^{18}F labeled fluoroethyl ether group as a replacement for the terminal alkyne, similar to derivatives 1a and 1c but derivative 1b does not have a modification to the crown ether. Finally, there is [^{18}F]icotinib derivative 1d, this derivative has a modification to the terminal alkyne, where a ^{18}F labeled 1,2,3-triazole scaffold replaced the terminal alkyne.

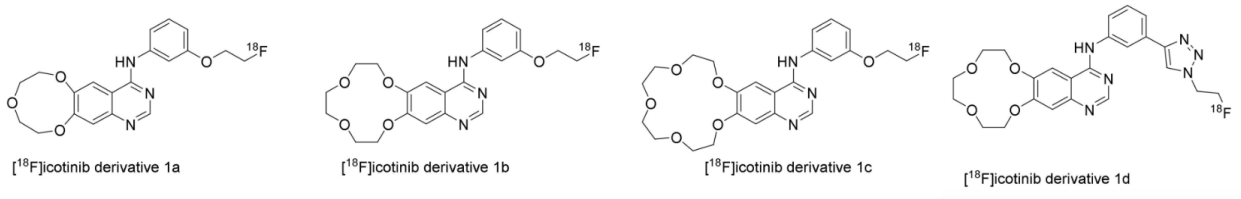

Figure 21: EGFR-TKI Tracers that are Analogues of Icotinib[34]

Afatinib is another drug that has been labeled using ^{18}F on the aniline ring, the structure can be seen in **Figure 22**. Studies done with this tracer show that there is no difference in uptake between the target and muscle which was used as the reference tissue.

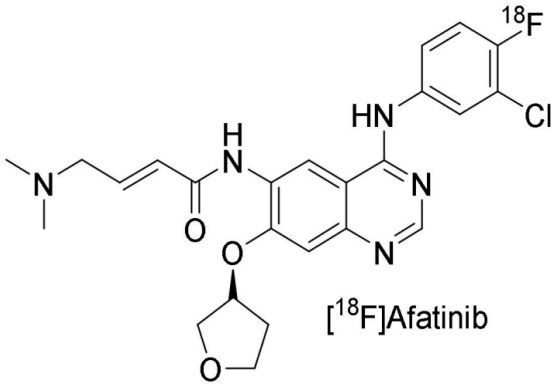

Figure 22: EGFR-TKI Tracer that is an Analogue of Afatinib[34]

3.2 RESULTS AND DISCUSSION

In reaction (a) from **Scheme 4**, 4-chloroquinazoline and 4-iodoaniline were reacted in isopropanol (iPrOH) at reflux (100°C) for 4 hours. The purpose of this reaction was to add the aromatic aniline to the quinazoline to build the scaffold for the fluorination. This reaction was successful in yielding the desired product, N-(4-iodophenyl)quinazolin-4-amine (**18**), in a high yield of 90%. Reaction success was confirmed using TLC, MS, proton nuclear magnetic

resonance (^{1}HNMR), carbon-13 nuclear magnetic resonance (^{13}CNMR), and infrared spectroscopy (IR). The reaction showed a new spot was formed on TLC that had a mass corresponding to the desired product **18**. The ^{1}H NMR and ^{13}C NMR confirmed the assigned structure of the product.

In reaction (b), a Sonogashira coupling reaction[32] was performed. Compound **18** was put in a flask with propargyl alcohol, bis(triphenylphosphine)palladium dichloride ($Pd(PPh_3)_2Cl_2$) and copper (I) iodide (CuI) in diethyl amine (Et_2NH). The purpose of this reaction was to cross couple propargyl alcohol to the aniline ring to form a new carbon-carbon bond in order to make a primary alcohol. This will allow us to create a good leaving group for successful fluorination. This reaction requires a palladium catalyst ($Pd(PPh_3)_2Cl_2$) and copper co-catalyst (CuI). This reaction was successful when stirred at room temperature under an inert atmosphere for 5 hours. The desired product of 3-{4-[(quinazolin-4-yl)amino]phenyl}prop-2-yn-1-ol (**19**) was successfully prepared with a yield of 48%. The TLC showed formation of product, LCMS showed a large peak with a mass that corresponds to the product in both the positive and negative spectra, both NMRs and IR confirmed the formation of the desired compound **19**.

In reaction (c), compound **19** was combined with p-toluenesulfonyl chloride (TsCl), and diisopropylethylamine (DIPEA) in dichloromethane (DCM). This reaction was cooled to 0^{o}C and stirred for 1 hour. The purpose of this reaction was to tosylate the hydroxyl group in order to make it a better leaving group for fluorination. This reaction was not successful, the reaction was monitored using TLC and LCMS and both experiments failed to show the formation of product, only starting material and TsCl could be identified. Since no product formed with the reaction at 0^{o}C the reaction was brought to room temperature to determine if temperature was a limiting factor. At room temperature the reaction was allowed to stir for 2 hours, the reaction was

monitored by TLC and LCMS. TLC and LCMS still failed to show any formation of product and only starting material and TsCl were identified. The conditions were modified to use pyridine as both the solvent and the base. It was stirred in an ice bath at 0^{o}C for 1 hour and then it was stirred at room temperature for 3 hours. This reaction was also unsuccessful as there was no indication that any product was being formed. This reaction was also done with trifluoromethanesulfonic anhydride (Tf_2O) instead of TsCl to attempt to use triflate as a leaving group for fluorination instead of a tosyl group. The reaction was done in both in DCM with DIPEA as the base and with pyridine acting as both the base and solvent. Both reactions were unsuccessful as well. Both TLC and LCMS failed to show consumption of starting material and formation of the desired product.

A different approach was taken to this synthesis, since the hydroxyl group could not be converted to a good leaving group after the Sonogashira reaction[32], the next approach was to prepare propargyl tosylate before performing the Sonogashira reaction. **Scheme 5** shows the second proposed synthetic route.

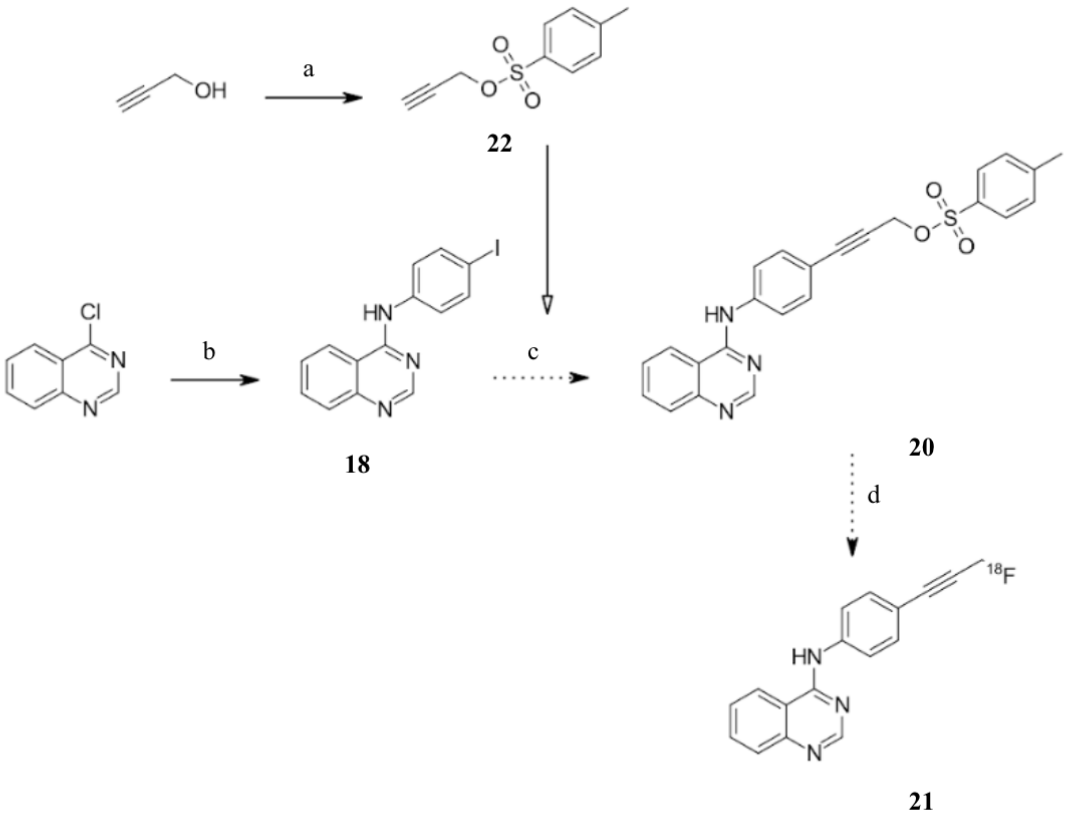

Scheme 5: Second proposed synthetic route for synthesis of the proposed Model System. (a) tosyl chloride, Et_2O, NaOH (b) 4-iodoaniline, isopropanol (c) propargyl tosylate, $Pd(PPh_3)_2Cl_2$, CuI, Et_2NH (d) KF, Kryptofix 2.2.2, CH_3CN

In reaction (a), propargyl tosylate was synthesized by reacting propargyl alcohol, TsCl, and sodium hydroxide (NaOH) in ether at 0°C with warming to room temperature overnight. When the reaction was finished TLC experiments showed formation of the product. ^{1}HNMR and ^{13}CNMR were used to confirm product formation. This reaction was successful in producing propargyl p-toluenesulfonate (**22**) with a yield of 91%. Reaction (b), yielding compound **18** is the same as in the original proposed synthetic scheme. Compound **22** was then reacted with **18** along with the palladium and copper co-catalysts in Et_2NH in the Sonogashira reaction (reaction (c)). This reaction was allowed to stir at room temperature for 1 hour. After 1 hour, TLC experiments show the absence of **22** and presence of starting material, there is no evidence of product

formation. It is proposed that **22** is not stable in the basic environment provided by Et_2NH and could therefore not be added to **18** to yield the desired tosylated product.

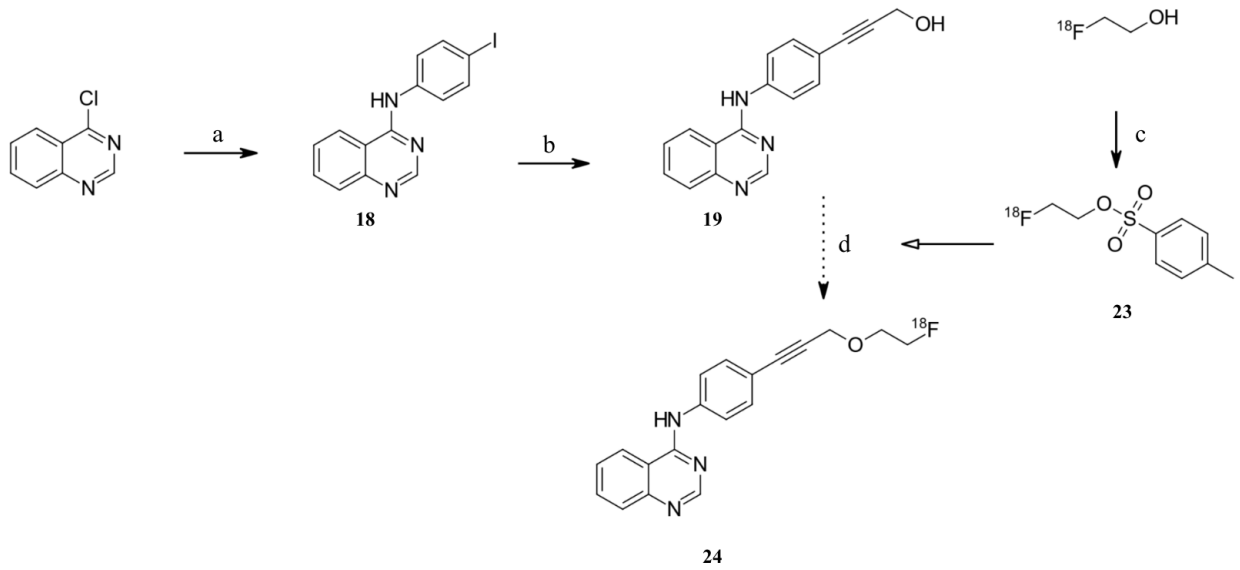

Scheme 6: Third proposed synthetic route for synthesis of the proposed Model System. (a) 4-iodoaniline, isopropanol (b) propargyl alcohol, $Pd(PPh_3)_2Cl_2$, CuI, Et_2NH (c) 2-fluoroethanol, TsCl, DIPEA, DMAP, DCM (d) fluoroethyl tosylate, K_2CO_3, DMSO

Scheme 6 depicts another approach to yield a fluorinated product. The difference between this product and the original proposed product is that there is a fluoroethyl ether group on the molecule instead of a fluorine. In this scheme, reactions (a) and (b) are the same as the original synthetic scheme and were both successful reactions. Reaction (c) is a reaction of 2-fluoroethanol with TsCl to yield 2-fluoroethyl p-toluenesulfonate (FEtTs). This reaction was carried out with DIPEA and 4-dimethylaminopyridine (DMAP) as bases in DCM, it was stirred at 0^oC and allowed to come to room temperature overnight. TLC and MS experiments done were able to prove the formation of product and absence of starting material. This reaction was successful in yielding FEtTs (compound **23**) with a yield of 1.512 g (81%). Compound **23** was then reacted with compound **19** in reaction (d) with K_2CO_3 as a base in DMSO, the reaction was allowed to stir for 1 hour at room temperature under inert atmosphere. After 1 hour, LCMS and

TLC experiments failed to show any formation of product. The reaction temperature was increased to 80°C and reacted for 1 hour, LCMS and TLC experiments still failed to show formation of any product. The reaction was then brought up to reflux temperature (200°C), after reacting for 2 hours the LCMS and TLC experiments still failed to show formation of product therefore this reaction was unsuccessful.

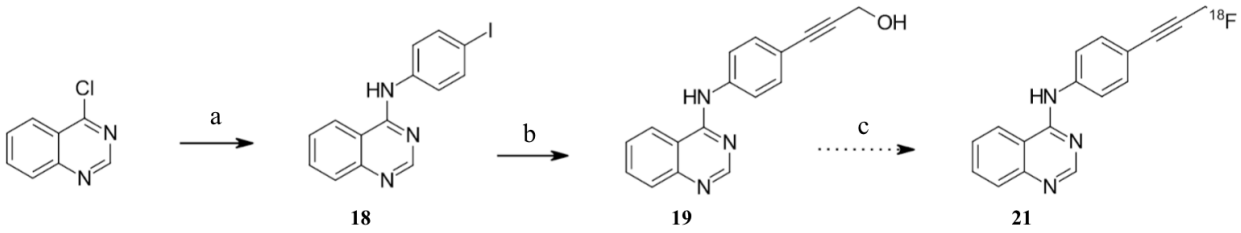

Scheme 7: Fourth proposed synthetic route for synthesis of the proposed Model System. (a) 4-iodoaniline, isopropanol (b) propargyl alcohol, $Pd(PPh_3)_2Cl_2$, CuI, Et_2NH (c) cesium fluoride, diisopropyl azodicarboxylate, triphenylphosphine, THF

Another attempt to successfully synthesize the desired product goes from compound **19** right to a fluorinated product without a tosylate intermediate. There are two reactions employed to see if it is possible to synthesize the fluorinated product. The first reaction seen in **Scheme 7** is a Mitsunobu reaction to replace the hydroxyl group with a fluorine using diisopropyl azodicarboxylate (DIAD), triphenylphosphine (PPh_3), and cesium fluoride (CsF). This reaction was done on ice at 0°C overnight. TLC experiments throughout the reaction time failed to show consumption of starting material and formation of product even after 24 hours. This reaction was deemed unsuccessful due to the lack of proof that the product was formed.

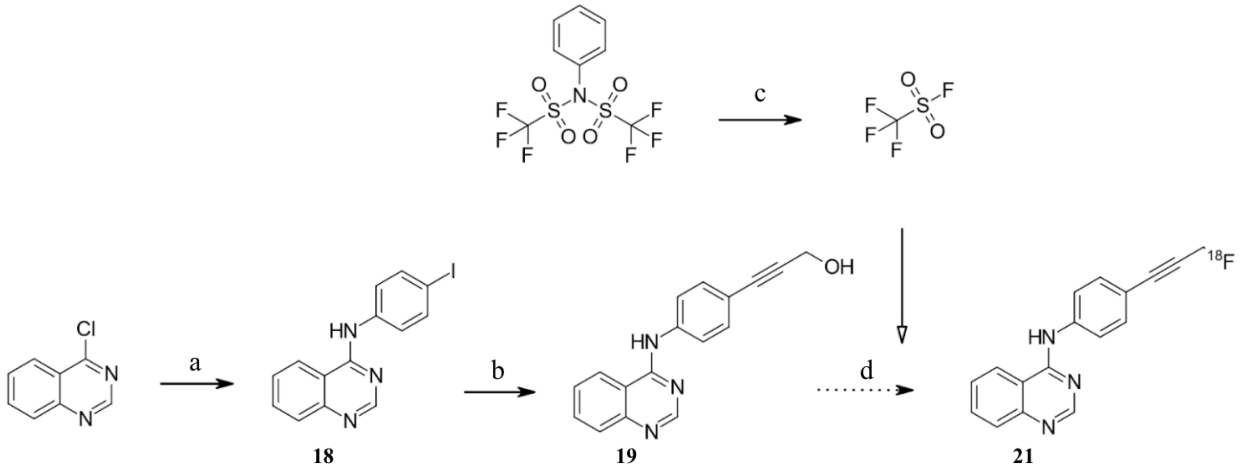

Scheme 8: Fifth proposed synthetic route for synthesis of the proposed Model System. (a) 4-iodoaniline, isopropanol (b) propargyl alcohol, $Pd(PPh_3)_2Cl_2$, CuI, Et_2NH (c) N,N-bis(trifluoromethylsulfonyl)aniline, lithium fluoride, DMF (d) 1,8-diazabicyclo(5.4.0)undec-7-ene, trifluoromethanesulfonyl fluoride, THF

The final reaction employed to attempt to synthesize the desired product happens by first making trifluoromethanesulfonyl fluoride (TfF) as a gas in one reaction and using that gas in a second reaction involving compound **19** and 1,8-diazabicyclo(5.4.0)undec-7-ene (DBU) which is a non-nucleophilic base. This reaction was done in two filter flasks connected by tubing to keep the gaseous TfF from escaping as the gas is forming it will flow through the tubing and dissolve in THF to react with compound **19**. This reaction was stirred at 60ºC with vigorous stirring for 2 hours. After 2hrs, MS and TLC experiments were performed and both experiments failed to show formation of product. This means that this reaction was also unsuccessful, and the fluorinated product cannot be formed.

This project has been unsuccessful, the synthesis strategies that were attempted have failed to produce any fluorinated product. In the reactions discussed in this chapter, a tosylation of a hydroxyl group was attempted using multiple strategies and these reactions were unable to produce the desired product. When the starting material was subjected to the reaction conditions and allowed to react there was no evidence of any product formation. When MS experiments

were performed after some reaction time all that could be identified was starting material in all cases. This suggests that the hydroxyl group was not getting deprotonated to initiate the addition of the tosyl group. It is unsure why the proton cannot be deprotonated because it is a primary hydroxyl group that is not sterically hindered, and the proton is an acidic proton which should allow it to be deprotonated. The first attempt was done with DIPEA and DMAP as bases in DCM. The starting material is not soluble in DCM and therefore the reaction couldn't progress due to solubility issues. The next attempted reaction used pyridine as both a solvent and base due to the fact that the starting material is soluble in pyridine, even with this approach, the hydroxyl group could not be deprotonated and only starting material could be identified. The reactions in which there was a direct conversion of the hydroxyl group to a fluorine were unsuccessful as well. After some reaction time, the only thing that could be identified by MS experiments was starting material. This suggests that the hydroxyl group is not able to be deprotonated by the DIAD in the Mitsunobu reaction to be replaced by the fluorine. The same thing can be seen with the TfF reaction, the hydroxyl group is not being deprotonated to allow for the addition of the triflate group and replacement of the fluorine. The other possible reason for the lack of success with these reactions is that the tosylated version of this molecule is not stable and it gets hydrolyzed back to starting material right away. The failure of multiple strategies suggests that more work needs to be done to be able to achieve a successful synthesis.

3.3 FUTURE WORK

This project still has the potential to be successful. More work needs to be done to find a suitable synthesis strategy to fluorinate this compound. The reactions attempted in this project could still be successful, one would need to consider different base and solvent combinations to allow the hydroxyl group to be deprotonated to allow for either the tosylation or displacement to

occur. One would also consider using extra dry solvents to avoid hydrolysis of the tosylate, this was not done as there was no access to extra dry solvents. The other way this synthesis could work is by doing the Sonogashira coupling then reducing the triple bond to a single bond through a hydrogenation reaction. Once this compound can be fluorinated using ^{19}F, it can then be fluorinated using ^{18}F and binding studies can be completed on this compound. The binding studies and cell assays will be used to determine the ability of this compound to be a successful tracer. Once this compound can be fluorinated, the successful synthesis approach can be applied to radiolabel EGFR-TKI drugs to be used in therapeutic outcome studies.

CHAPTER 4: SYNTHESIS OF ^{18}F ERLOTINIB

4.1 PROPOSED SYNTHESIS

Chapter 1.1.3 discusses first- and second-generation EGFR-TKIs, how they are used to treat EGFR mutation positive cancers, and how resistance develops to these drugs. Using the synthetic strategy proposed in Chapter 3, a single protocol can be developed to make ^{18}F derivatives of all clinically available EGFR-TKIs. An ^{18}F analogue will first be made for the drug Erlotinib. Erlotinib is a first-generation EGFR-TKI anticancer drug that is taken orally to treat EGFR mutation positive cancers. **Figure 23** shows the structure of the proposed erlotinib analogue, and **Scheme 9** shows the proposed synthetic route to synthesize the desired ^{18}F labeled product (compound **28**).

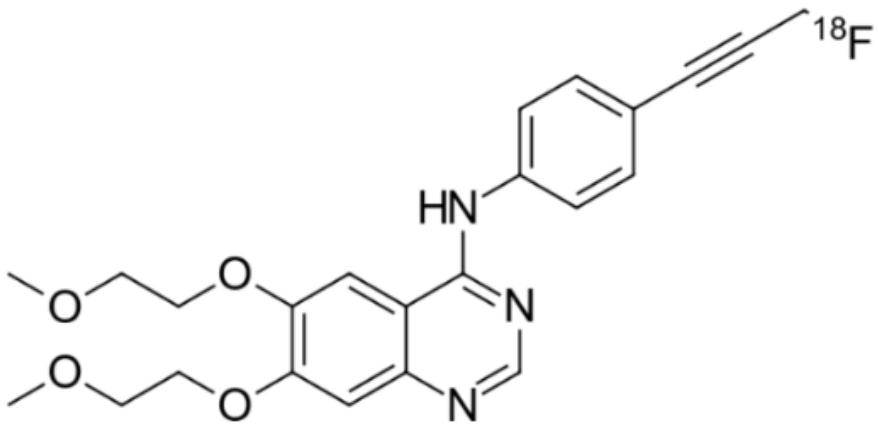

Figure 23: Proposed Structure of an ^{18}F labeled Analogue of the First-Generation EGFR-TKI Erlotinib

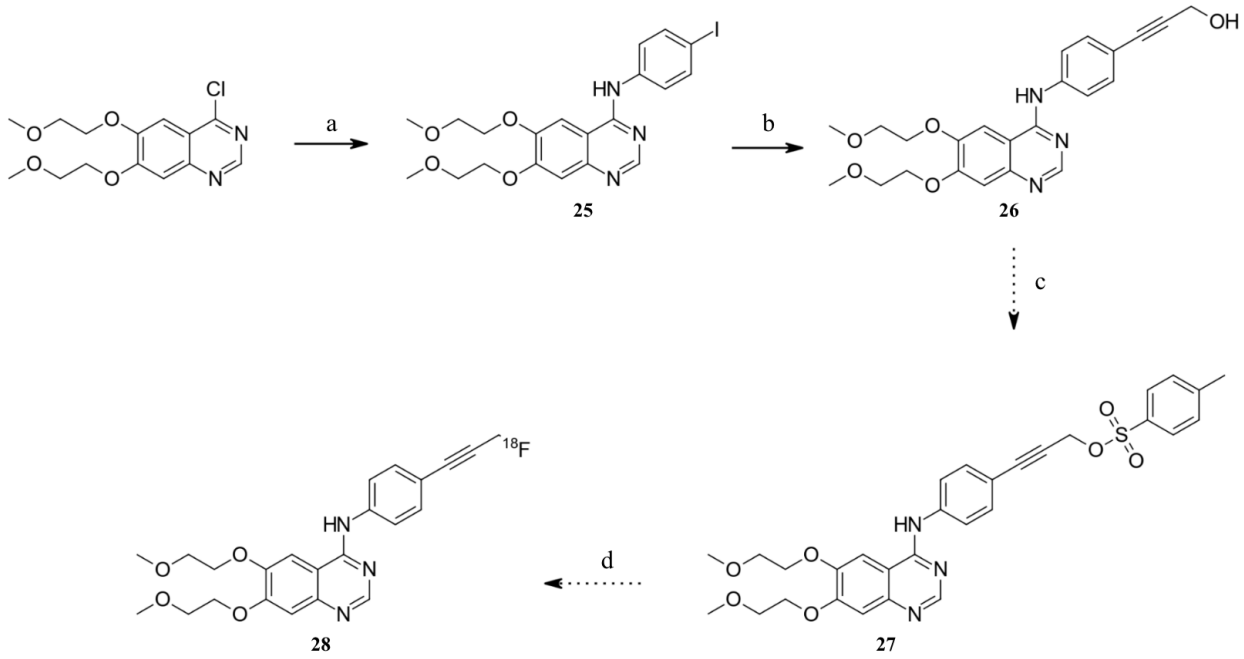

Scheme 9: Proposed synthetic route for synthesis of the proposed ^{18}F analogue of erlotinib. (a) 4-iodoaniline, isopropanol (b) propargyl alcohol, $Pd(PPh_3)_2Cl_2$, CuI, Et_2NH (c) p-toluenesulfonylchloride, DIPEA, DCM (d) KF, Kryptofix 2.2.2, CH_3CN

4.2 RESULTS AND DISCUSSION

In reaction (a), 4-iodoaniline was reacted with 4-chloro-6,7-bis(2-methoxyethoxy)-quinazoline in iPrOH at reflux for 4 hours to yield compound **25**, N-(4-iodophenyl)-6,7-bis(2-methoxyethoxy)quinazolin-4-amine. This reaction is the same reaction seen in the model system synthesis and the purpose of this reaction is to build the scaffold of EGFR-TKI drugs that will be used for the radiolabelling steps. LCMS and TLC experiments show formation of product and absence of starting material; ^{1}HNMR and ^{13}CNMR experiments confirmed the structure of the desired product. This product was formed with a yield of 81%.

In reaction (b), compound **25** was used in the Sonogashira reaction seen in the model system synthesis. It was put in a flask equipped with Et_2NH and propargyl alcohol. The co-catalysts used are $Pd(PPh_3)_2Cl_2$ and CuI and the reaction happened under an inert atmosphere at room temperature for 5 hours. The purpose of this reaction is the same as with the model system

synthesis, to create a new carbon-carbon bond to introduce a primary alcohol to make into a better leaving group for fluorination. Throughout the reaction LCMS and TLC experiments were performed, these experiments showed the formation of product and consumption of starting material. ^{1}HNMR and ^{13}CNMR experiments were able to confirm the structure of the desired product, compound **26**. This reaction was successful in yielding compound **26** with a yield of 75%.

This part of the project was performed at the same time as the model system synthesis. Each time there was a successful reaction in the model system synthesis, the same reaction was performed to synthesize the ^{18}F erlotinib analogue. This was done because the starting material for the ^{18}F erlotinib synthesis was a lot more expensive than the starting material for the model system synthesis. Due to the lack of success in Chapter 3 to produce a fluorinated product and time constraints, reactions (c) and (d) were not attempted. This synthesis still has the potential to be successful. As mentioned in Chapter 3, the tosylation and fluorination reactions may not be able to proceed due to solubility issues. Compound **26** does not have as many solubility issues as Compound **19** and therefore there may be a higher chance that the tosylated or fluorinated product can be synthesized. The addition of the methoxyethoxy groups may also help with the ability of the primary hydroxyl group to be deprotonated and therefore these reactions do need to be attempted with Compound **26**.

CHAPTER 5: EXPERIMENTAL

5.1 GENERAL EXPERIMENTAL TECHNIQUES, INSTRUMENTS AND MATERIALS

All reagents were purchased from Sigma-Aldrich, Fisher Scientific or Chem Impex and used without further purification with the following exceptions:

1. 4-Iodoaniline was purified by recrystallization with ethanol
2. p-Toluenesulfonyl chloride was purified by dissolving it in a minimal amount of chloroform then diluting it with petroleum ether using 5x the volume of chloroform used, the resulting solution was filtered by vacuum filtration and the solvent was removed by rotary evaporation.

NMR spectra were collected on a 500 MHz Bruker Advance Neo spectrometer with SmartProbe and processed using Bruker Topspin 4 software or on a 500 MHz Varian UNITY INOVA NMR spectrometer system, VNMR 6.1C software at room temperature. Chemical shifts are reported in parts per million (ppm) from an internal standard of tetramethylsilane (TMS). The NMR data are reported as follows: chemical shift multiplicity, coupling constant in Hertz, integration.

Mass spectra data were obtained using an Advion Expression CMS spectrometer operated in atmospheric pressure chemical ionization mode (APCI) unless otherwise specified.

Infrared (IR) spectra data was obtained using a Perkin Elmer 1320 IR Spectrometer with a resolution of 1 cm^{-1}. All spectra were determined without solvent (neat) in the transmission mode and reported as wavenumbers (cm^{-1}).

Liquid Chromatography Mass Spectrometry (LCMS) data obtained using Agilent 6120 Single Quadrupole LC/MS using electrospray ionization.

Column chromatography was carried out using SiliaFlash P60 40-63 μm (230-400 mesh) silica gel with a mixture of hexane and ethyl acetate unless otherwise stated.

5.2 PREPARATION OF PRODUCTS

5.2.1 PREPARATION OF PRODUCTS IN CHAPTER 2

Ethyl 3-hydroxy-4-(2-methoxyethoxy)benzoate (**1**)

Sodium hydride, 60% in mineral oil, (NaH) (339 mg, 14.1 mmoles) was added to a 250 mL round bottom flask equipped with a stir bar. Hexane was added to remove the mineral oil from the NaH. The hexane was removed using a Pasteur pipette, this was repeated 3 times. Dimethylformamide (100 mL) was added, and the flask was flushed with nitrogen gas. Protocatechuic acid ethyl ester (999 mg, 5.48 mmoles) was dissolved in dimethylformamide (10 mL) and added slowly to the flask using a syringe. The reaction mixture was allowed to stir for 15 minutes. 1-bromo-2-methoxyethane (599 μL, 6.03 mmoles) was added to the reaction mixture and stirred at room temperature for 24 hours. TLC and MS indicated no product formation therefore nothing further was done to the reaction.

Ethyl 3-hydroxy-4-(2-methoxyethoxy)benzoate (**1**)

Protocatechuic acid ethyl ester (711 mg, 3.90 mmoles) was dissolved in acetonitrile (50 mL) in a 100 mL round bottom flask equipped with a stir bar followed by the addition of potassium carbonate (585 mg, 4.23 mmoles). The mixture was stirred at reflux for 1 hour then 1-bromo-2-methoxyethane (419 μL, 4.22 mmoles) was added and the reaction was stirred at reflux for 24 hours. Once the reaction was complete, acetonitrile was evaporated using rotary evaporation. Ethyl acetate (100 mL), distilled water (100 mL) and of 10% HCl (50 mL) was added to the flask. The ethyl acetate layer was washed twice with water then dried using magnesium sulfate

and the ethyl acetate was removed using rotary evaporation. Isolation was attempted using column chromatography. The mono- and dialkylated products were unable to be separated, resubjection to the reaction conditions did not change product ratio. Monoalkylated: MS m/z: $[M+H]^+$ calculated for $C_{12}H_{16}O_5^+$: 241.33, found 241.2, $[M-H]^-$ $C_{12}H_{16}O_5^-$: 239.33, found 239.1. Dialkylated: MS m/z: $[M+H]^+$ calculated for $C_{15}H_{22}O_6^+$: 299.33, found 299.3.

Ethyl 3-hydroxy-4-(2-methoxyethoxy)benzoate (**1**)

Protocatechuic acid ethyl ester (970 mg, 5.32 mmoles) was dissolved in acetonitrile (50 mL) in a 100 mL round bottom flask equipped with a stir bar. Lithium carbonate (1.018 g, 13.78 mmoles) was added to the flask. The mixture was heated to 80ºC for 1 hour then 1-bromo-2-methoxyethane (1.36 mL, 10.25 mmoles) was added and the reaction was stirred on heat (80ºC) for 5 days. Once the reaction was complete, the reaction mixture was diluted with distilled water (100 mL) and 10% HCl (50 mL). The mixture was extracted with ether and washed with water 2 times then dried using magnesium sulfate. The excess ether was removed using rotary evaporation and isolation was performed using column chromatography. MS m/z: $[M+H]^+$ calculated for $C_{15}H_{22}O_6^+$: 241.33, found 241.2, $[M-H]^-$ $C_{15}H_{22}O_6^-$: 239.33, found 239.1; The monoalkylated product was isolate but found to be approximately a 1:1 mixture of the 2 monoalkylated regioisomers.

Ethyl 3,4-bis(acetyloxy)benzoate (**9**)

Protocatechuic acid ethyl ester (980 mg, 5.37 mmoles) was dissolved in 50 mL of pyridine in a 100 mL round bottom flask equipped with a stir bar. Acetic anhydride (1.50 mL, 15.86 mmoles) was added to the flask. The reaction was stirred at room temperature for 24 hours. Once the reaction was complete, it was diluted with 200 mL of distilled water. The mixture was extracted with 100 mL of ethyl acetate. The ethyl acetate was washed with 100 mL of distilled water, then

100 mL of 10% hydrochloric acid, then a solution of copper sulfate (10 g of copper sulfate in 100 mL of water), and finally 100 mL of saturated sodium bicarbonate solution. The excess ethyl acetate was removed via rotary evaporation and isolation was attempted using column chromatography. The mono- and diacetylated products could not be separated, resubjection to reaction conditions did not change product ratio. Monoacetylated: MS m/z: $[M+H]^+$ calculated for $C_{11}H_{12}O_5^+$: 224.21, found 225.1, $[M-H]^-$ $C_{12}H_{16}O_5^-$: 239.33, found 239.1. Diacetylated: MS m/z: $[M+H]^+$ calculated for $C_{13}H_{14}O_6^+$: 266.25, found 267.1.

5.2.2 PREPARATION OF PRODUCTS IN CHAPTER 3

N-(4-iodophenyl)quinazolin-4-amine (**18**)[35]

4-chloroquinazoline (120 mg, 0.73 mmoles) was put into a 50 mL round bottom flask equipped with a stir bar and approximately 25 mL of isopropanol. 4-iodoaniline (180 mg, 0.82 mmoles) was added to the flask. The flask was covered in aluminum foil and the reaction mixture was heated to reflux using a heating block and allowed to stir for 4 hours. The resulting mixture was filtered using vacuum filtration to isolate the solid. The solid was washed with isopropanol and allowed to air dry overnight. This resulted in a green solid with a yield of 235 mg (93%). MS m/z: $[M+H]^+$ calculated for $C_{14}H_{10}N_3I^+$: 348.15, found 348.0; ^{1}H NMR (500MHz, DMSO) δ (ppm): 11.47 (s, 1H), 8.95 (s, 1H), 8.82 (d, J=8.3 Hz, 1H), 8.11 (t, J=7.3 Hz, 1H), 7.94 (d, J=8.3, 1H), 7.89 (t, J=7.6, 1H) 7.86 (d, J=8.6 Hz, 2H), 7.59 (d, J=8.6 Hz, 2H); ^{13}C NMR (125.8 MHz, DMSO) δ (ppm): 160.2, 151.6, 139.5, 138.0, 137.1, 136.7, 129.1, 127.3, 125.3, 120.5, 114.1, 92.2; IR (neat): 3398 cm^{-1}.

3-{4-[(quinazolin-4-yl)amino]phenyl}prop-2-yn-1-ol (**19**)[32]

N-(4-iodophenyl)quinazoline-4-amine (260 mg, 0.75 mmoles) was put into a 50 mL round bottom flask equipped with a stir bar and approximately 25 mL of diethylamine. Propargyl

alcohol (65 μL, 1.12 mmoles) was added to the flask, the flask was flushed with argon gas and kept under an inert atmosphere. Bis(triphenylphosphine)palladium dichloride (102 mg, 0.15 mmoles) and copper iodide (17 mg, 0.089 mmoles) were added to the flask. The flask was covered with aluminum foil and the reaction was allowed to stir at room temperature for 5 hours. The resulting mixture was filtered using vacuum filtration to isolate the solid, the solid was washed with ethanol and allowed to air dry overnight. This resulted in a white solid with a yield of 100 mg (48%). MS m/z: $[M+H]^+$ calculated for $C_{17}H_{13}N_3O^+$: 276.30, found 276.0; ^{1}H NMR (500MHz, DMSO) δ (ppm): 9.90 (s, 1H), 8.65 (s, 1H), 8.57 (d, J=8.3 Hz, 1H) 7.96 (d, J=8.6 Hz, 2H), 7.86 (t, J=7.7 Hz, 1H), 7.82 (d, J=1.7 Hz, 1H), 7.67 (t, J=7.7 Hz, 1H), 7.46 (d, J=8.7 Hz, 2H), 5.33 (t, J=6.0 Hz, 1H), 4.31 (d, J=6.0 Hz, 2H); ^{13}C NMR (125.8 MHz, DMSO) δ (ppm): 157.9, 154.8, 150.2, 140.0, 133.7, 132.1, 128.4, 126.9, 123.5, 122.2, 117.5, 115.7, 89.7, 84.2, 50.0.

Propargyl p-toluenesulfonate (**22**) [33]

Propargyl alcohol (4.86 g, 8.66 mmoles), TsCl (20.07 g, 105.27 mmoles), and approximately 125 mL of diethyl ether (Et_2O) were added to a 250 mL round bottom flask equipped with a mechanical stir bar. The flask was put under an inert atmosphere using argon gas and cooled on an ice bath to 0°C. Sodium hydroxide (NaOH) pellets (17.59g, 439.97 mmoles) were added to the solution in 7 portions with vigorous stirring. After approximately an hour the flask was taken off the ice bath and allowed to warm to room temperature and stirred for 24 hours. The resulting solution was poured into cold water, the Et_2O was collected, and the aqueous layer was extracted with 100 mL of Et_2O twice. The Et_2O layers were combined and dried using sodium sulfate (Na_2SO_4) then the excess Et_2O was evaporated using rotary evaporation. This resulted in a yellow oil with a yield of 18.22g (91%). $[M\text{-}CH_2CCH]^-$ calculated for $C_7H_7O_3^-$: 170.96, found

170.9; ^{1}H NMR (500MHz, $CDCl_3$) δ (ppm): 7.71 (d, J=7.0 Hz, 2H), 7.26 (d, J=6.7 Hz, 2H), 4.60 (d, J=2.1 Hz, 2H), 2.42 (t, J=2.1 Hz, 1H), 2.36 (s, 3H); ^{13}C NMR (125.8 MHz, DMSO) δ (ppm): 145.7, 132.8, 130.6, 128.2, 80.6, 80.0, 65.40, 58.7.

2-Fluoroethyl p-Toluenesulfonate (**23**)

Fluoroethanol (0.5 mL, 8.58 mmoles) was put into a 100 mL round bottom flask equipped with a stir bar and approximately 50 mL of dichloromethane. Dimethylamino pyridine (210 mg, 1.71 mmoles), diisopropylethylamine (2.25 mL, 17.4 mmoles) was added to the flask and the flask was cooled to 0^{o}C and flushed with argon gas. p-Toluenesulfonyl chloride (2.523 g, 13.2 mmoles) was added to the flask, the reaction mixture was stirred and allowed to climb to room temperature over 18 hours. The reaction was poured into a separatory funnel and washed with 10% HCl (100 mL), then it was washed with water (100 mL) twice. The organic layer was then dried using $MgSO_4$ then the DCM was evaporated using rotary evaporation, and the crude product was purified using column chromatography. This resulted in a colourless oil with yield of 1.512 g (81%). MS m/z: $[M+H]^+$ calculated for $C_9H_{11}O_3FS^+$: 219.25, found 219.2. ^{1}H NMR (500MHz, $CDCl_3$) δ (ppm): 7.70 (d, J=7.1 Hz, 2H), 7.26 (d, J=6.7 Hz, 2H), 4.46 (dt, J=39.3, 3.5 Hz, 2H), 4.16 (dt, J=22.7, 3.5 Hz, 2H), 2.35 (s, 3H). ^{13}C NMR (125.8 MHz, DMSO) δ (ppm): 145.6, 132.6, 130.6, 128.1, 81.5 (J=163.5), 70.1 (J=20.1), 60.2. IR (neat): 2960, 1177, 1358 cm^{-1}.

5.2.3 PREPARATION OF PRODUCTS IN CHAPTER 4

N-(4-iodophenyl)-6,7-bis(2-methoxyethoxy)quinazolin-4-amine (**25**)[35]

4-chloro-6,7-bis(2-methoxyethoxy)quinazoline (513 mg, 1.64 mmoles) was put into a 100 mL round bottom flask equipped with a stir bar and approximately 50 mL of isopropanol and 4-iodoaniline (430 mg, 1.96 mmoles) was added to the flask. The flask was covered in aluminum foil and the reaction mixture was heated to reflux using a heating block and allowed to stir for 2

hours. The resulting mixture was filtered using vacuum filtration to isolate the solid. The solid was washed with isopropanol and allowed to air dry overnight. This resulted in a while solid with a yield of 653 mg (81%). MS m/z: $[M+H]^+$ calculated for $C_{20}H_{21}N_3O_4I^+$: 496.31, found 496.3, $[M-H]^-$ $C_{20}H_{21}N_3O_4I^-$: 494.31, found 494.1; ^{1}H NMR (500MHz, DMSO) δ (ppm): 8.81 (s, 1H), 8.20 (s, 1H), 7.84 (d, J=8.7 Hz, 2H), 7.55 (d, J=8.7, 2H), 7.32 (s, 1H), 4.32-4.36 (m, 4H), 3.75-3.81 (m, 4H), 2x OCH_3 obscured by residual water in DMSO; ^{13}C NMR (125.8 MHz, DMSO) δ (ppm): 156.4, 154.1, 153.2, 148.6, 147.5, 140.3, 132.0, 122.1, 117.1, 109.5, 108.7, 103.7, 89.5, 84.3, 70.5, 68.9, 68.5, 58.8, 50.0; IR (neat): 1506 cm^{-1}.

3-{4-[(quinazolin-4-yl)amino]phenyl}prop-2-yn-1-ol (**26**)[32]

N-(4-iodophenyl)-6,7-bis(2-methoxyethoxy)quinazolin-4-amine (**25**) (206 mg, 0.416 mmoles) was put into a 50 mL round bottom flask equipped with a stir bar and approximately 25 mL of diethylamine. Propargyl alcohol (50 μL, 0.89 mmoles) was added to the flask, the flask was flushed with argon gas and kept under an inert atmosphere. Bis(triphenylphosphine)palladium dichloride (66 mg, 0.094 mmoles) and copper iodide (12 mg, 0.063 mmoles) were added to the flask. The flask was covered with aluminum foil and the reaction was allowed to stir at room temperature for 5 hours. The resulting mixture was filtered using vacuum filtration to isolate the solid, the solid was washed with ethanol and allowed to air dry overnight. This resulted in a while solid with a yield of 176 mg (75%). MS m/z: $[M+H]^+$ calculated for $C_{23}H_{25}N_3O_5^+$: 424.46, found 424.5, $[M-H]^-$ $C_{23}H_{25}N_3O_5^-$: 422.46, found 421.5; ^{1}H NMR (500MHz, DMSO) δ (ppm): 5.42 (s, 1H), 8.50 (s, 1H), 7.88 (d, J=8.6 Hz, 2H), 7.87 (s, 1H), 7.45 (d, J=8.6 Hz, 2H), 7.23 (s, 1H), 5.32 (s, 1H), 4.26-4.32 (m, 6H), 3.76-3.80 (m, 2H), 3.76-3.73 (m, 2H), 3.37 (s, 3H), 3.35 (s, 3H); ^{13}C NMR (125.8 MHz, DMSO) δ (ppm): 158.4, 156.1, 149.8, 149.5, 137.9, 139.3, 127.2, 107.9, 105.3, 91.6, 70.6, 70.5, 69.3, 58.9; IR (neat): 3381, 3173, 2912, 1514 cm^{-1}.

REFERENCES

1. Creative Diagnostics (2022). EGF/EGFR Signalling Pathway. Retrieved from: https://www.creative-diagnostics.com/egf-egfr-signalling-pathway.htm on May 2, 2022.
2. De Bono, S. and Rowinsky, E. (2002). The ErbB receptor family: a therapeutic target for cancer. *Trends Mol. Med.* 8(4):S19-S26.
3. Bethune, G. Bethune, D. Ridgeway, N. and Xu, Z. (2010). Epidermal growth factor receptor (EGFR) in lung cancer: an overview and update. *J Thorac. Dis.* 2(1):48-51.
4. Herbst, R.S. (2004). Review of epidermal growth factor receptor biology. *Int J. Radiation Biol. Phys.* 59(2):21-26.
5. Seshacharyulu, P. Ponnusamy, M. Haridas, D. Jain, M. Ganti, A. and Batra, S. (2012). Targeting the EGFR signalling pathway in cancer therapy. *Expert Opin. Ther. Targets.* 16(1):15-31.
6. Research Collaboratory for Structural Bioinformatics. (2002). Crystal structure of the complex of human epidermal growth factor receptor and receptor extracellular domains. Retrieved from: https://www.rcsb.org/structure/1IVO on May 2, 2022.
7. YASARA. (1993). Yet another scientific artificial reality application. Retrieved from: www.yasara.org on May 2, 2022.
8. Bogden, S. and Klämbt, C. Epidermal growth factor receptor signalling. *Curr. Biol.* 10(8):R292-R295.
9. Bethesda (MD), National Institutes of Health (US). (2007). Understanding cancer. *NIH Curriculum Supplement Series*. Retrieved from: https://www.ncbi.nlm.nih.gov/books/NBK20362/ on May 2, 2022.

10. Meegan, M.J. and O'Boyle, N. (2019). Special issue "anticancer drugs". *Pharmaceuticals.* 12(3):134.

11. Nan, X. Xie, C. Yu, X. and Liu, J. (2017). EGFR TKI as first-line treatment for patients with advanced EGFR mutation-positive non-small cell lung cancer. *Oncotarget.* 8(43):75712-75726.

12. Sasaki, T. Kuniyasu, H. and Yamashita, Y. (2013). The role of epidermal growth factor receptor in cancer metastasis and microenvironment. *Biomed Res Int.* 2013:546318.

13. Tang, J. Salama, R. Gadgeel, S.M. Fazlul S.H. and Ahmad, A. (2013). Erlotinib resistance in lung cancer: current progress and future perspectives. *Front Pharmacol.* 4(15):1-9.

14. Zhang, H. (2016). Three generations of epidermal growth factor receptor tyrosine kinase inhibitors developed to revolutionize the therapy of lung cancer. *Drug Des Devel Ther.* 10:3867-3872.

15. Kujtan, L. and Subramanian, J. (2019). Epidermal growth factor receptor tyrosine kinase inhibitors for the treatment of non-small cell lung cancer. *Expert Rev. Anticancer Ther.* 19(7):547-559.

16. Rosell, R. Morán, T. Carcereny, E. Quiroga, V. Molina M.A. Costa, C. Benlloch, S. Tarón, M. (2010). Non-small cell lung cancer harbouring mutations in the EGFR kinase domain. *Clin Transl Oncol.* 12:75-80.

17. Takeda, M. and Nakagawa, K. (2019). First and second generation EGFR-TKIs are all replaced to osimertinib in chemo-naive EGFR mutation-positive non-small cell lung cancer. *Int. J. Mol. Sci.* 20(1):146.

18. Rebuzzi, S. Alfieri, R. La Monica, S. Minati, R. Petronini, P.G. and Tiseo, M. (2020). Combination of EGFR-TKIs and chemotherapy in advanced EGFR mutated NSCLC: review of the literature and future perspectives. *Crit Rev Oncol Hematol.* 146:102820.

19. Verma, N. Rai, A.K. Kaushik, V. Brünnert, D. Chahar, K.R. Pandey, J. and Goyal, P. (2016). Identification of gefitinib off-targets using a structure-based systems biology approach; their validation with reverse docking and retrospective data mining. *Sci. Rep.* 6:1-12

20. Saha, G.B. (2010). Fundamentals of nuclear pharmacy. Springer New York, NY.

21. Keith, S. Doyle, J.R. Harper, C. Mumtaz, M. Tarrago, O. Wohlers, D.W. Diamond, G.L. Citra, M. and Barber, L.E. (2012). Toxicological profile for radon. Agency for Toxic Substances and Disease Registry, Atlanta, GA.

22. Tafti, D. and Banks, K.P. (2022). Nuclear medicine physics. StatPearls Publishing, Treasure Island, Fluorida.

23. Connor, N. (2019). What is decay constant - definition. Retrieved from: https://www.radiation-dosimetry.org/what-is-decay-constant-definition/ on May 3, 2022.

24. Peach, K. Wilson, P. and Jones, B. (2011). Accelerator science in medical physics. *Br. J. Radiol.* 84(1):S004-S010.

25. El-Saftawy, A.A. (2013). Regulating the performance parameters of accelerated particles.

26. Jacobson, O. Kiesewetter, D.O. and Chen, X. (2015). Fluorine-18 radiochemistry, labeling strategies and synthetic routes. *Bioconjug Chem.* 26(1):1-18.

27. National Research Council and Institute of Medicine Committee on the Mathematics and Physics of Emerging Dynamic Biomedical Imaging. (1996). Mathematics and physics of emerging biomedical imaging. National Academies Press, Washington, DC.

28. Shukla, A.K. and Kumar, U. (2006). Positron emission tomography: an overview. *J. Med. Phys.* 31(1):13-21.

29. Vaalburg, W., and Brady, F. (1995). Radiolabelled Anticancer Drugs for In vivo Pharmacokinetic Studies by PET. In: Comar, D. (eds) PET for Drug Development and Evaluation. Developments in Nuclear Medicine, vol 26. Springer, Dordrecht.

30. Anand, S.S. Singh, H, and Dash, A.K. (2009). Clinical applications of PET and PET-CT. *Med J Armed Forces India.* 65(4):353-358.

31. Zhang, Y. Tortorella, M. Liao, J. Qin, X. Chen, T. Luo, J. Guan, J. Talley, J.J. and Tu, Z. (2015). Synthesis and evaluation of novel erlotinib-NSAID conjugates as more comprehensive anticancer agents. *ACS Med. Chem. Lett.* 6:1086-1090.

32. Sonogashira, K. Tohda, Y. and Hagihara, N. (1975). A convenient synthesis of acetylenes: catalytic substitutions of acetylenic hydrogen with bromoalkenes, iodoarenes, and bromopyridines. *Tetrahedron Lett.* 50:4467-4470.

33. Zhang, Q. Ren, H. Baker, G.L. (2014). An economical and safe procedure to synthesize 2-hydroxy-4-pentynotic acid: a precursor towards 'clickable' biodegradable polylactide. *Beilstein J. Org. Chem.* 10:1365-1371.

34. Högnäsbacka, A. Poot, A.J. Vugts, D.J. van Dongen, G.A.M.S. and Windhorst, A.D. (2022). The development of positron emission tomography tracers for in vivo targeting the kinase domain of the epidermal growth factor receptor. *Pharmaceuticals.* 15(450):1-35.

35. Breza, N. Pató, J. Örfi, L. Hehymegi-Barakonyi, B. Bánhegyi, P. Várkondi, E. Borbély, G. Peták, I. and Kéri, G. (2008). Synthesis and characterization of novel quinazoline type inhibitors for mutant and wild-type EGFR and RICK kinases. *J. Recept. Signal Transduct.* 28(4):361-373.